IZMIR KATIP CELEBI UNIVERSITY

GRADUATE SCHOOL OF NATURAL AND APPLIED SCIENCES

DEVELOPMENT OF MICROSTRUCTURAL AND MECHANICAL PROPERTIES OF ALUMINUM ALLOYS BY EQUAL CHANNEL ANGULAR PRESSING (ECAP) PROCESS

M.Sc. THESIS

Mehmet Mahsun YEŞİL

Department of Materials Science and Engineering

JULY 2018

IZMIR KATIP CELEBI UNIVERSITY

GRADUATE SCHOOL OF NATURAL AND APPLIED SCIENCES

DEVELOPMENT OF MICROSTRUCTURAL AND MECHANICAL PROPERTIES OF ALUMINUM ALLOYS BY EQUAL CHANNEL ANGULAR PRESSING (ECAP) PROCESS

M.Sc. THESIS

Mehmet Mahsun YEŞİL
(Student No. Y120111011)

Department of Materials Science and Engineering

Thesis Advisor: Assoc. Prof. Dr. Mücahit SÜTÇÜ

Thesis Co-Advisor: Dr. Ebubekir ATAN

JULY 2018

İZMİR KATİP ÇELEBİ ÜNİVERSİTESİ
FEN BİLİMLERİ ENSTİTÜSÜ

EŞ KANAL AÇILI PRESLEME (EKAP) YÖNTEMİYLE ALUMİNYUM ALAŞIMLARININ MİKROYAPI VE MEKANİK ÖZELLİKLERİNİN GELİŞTİRİLMESİ

YÜKSEK LİSANS TEZİ

Mehmet Mahsun YEŞİL
(Öğrenci No. Y120111011)

Malzeme Bilimi ve Mühendisliği Anabilim Dalı

Tez Danışmanı: Doç. Dr. Mücahit SÜTÇÜ

Tez Eş Danışmanı: Dr. Öğr.Üyesi Ebubekir ATAN

TEMMUZ 2018

Mehmet Mahsun YEŞİL, a **M.Sc.** student of **IKCU Graduate School Of Natural And Applied Sciences**, successfully defended the thesis entitled "**DEVELOPMENT OF MICROSTRUCTURAL AND MECHANICAL PROPERTIES OF ALUMINUM ALLOYS BY EQUAL CHANNEL ANGULAR PRESSING (ECAP) PROCESS** ", which he prepared after fulfilling the requirements specified in the associated legislations, before the jury whose signatures are below.

Thesis Advisor :

           Assoc. Prof. Dr. Mücahit SÜTÇÜ   ....
           İzmir Katip Çelebi University

Jury Members :

           Dr. Onur ERTUĞRUL   ....
           İzmir Katip Çelebi University

           Dr. Mustafa EROL   ....
           Dokuz Eylül University

Date of Submission : 30.06.2018
Date of Defense   : 20.07.2018

To my family; my wife, doughters and son.

FOREWORD

First and foremost, I would like to thank my advisor **Assoc. Prof. Dr. Mücahit SÜTÇÜ** and co-advisor **Dr. Ebubekir ATAN** for their guidance, wisdom and constructive critiques.

I want to express my special thanks to **Assoc. Prof. Dr. Mehmet ÇEVİK** and his team for clarifying and facilitating the procedures and perspectives.

I would also like to thank Jury Members **Dr. Onur ERTUĞRUL** and **Dr. Mustafa EROL** for their realistic and sophisticated criticism.

Thanks go to **Mr. Mesut ÖZER** and **Mr. Saadet GÜLER** for their supports during laboratory studies and tests.

I am also thankful to **Mrs. Selin KAYA** for her support with sharing valuable documentation and material setup efforts.

July 2018   Mehmet M.Yeşil

TABLE OF CONTENTS

ABBREVIATIONS

SPD   **:** Severe Plastic Deformation
ECAP   **:** Equal Channel Angular Pressing
UFG   **:** Ultra-Fine Grained
GB   **:** Grain Boundary
LAGB   **:** Low Angle Grain Boundaries

LIST OF TABLES

Page

LIST OF FIGURES

DEVELOPMENT OF MICROSTRUCTURAL AND MECHANICAL PROPERTIES OF ALUMINUM ALLOYS BY EQUAL CHANNEL ANGULAR PRESSING (ECAP) PROCESS

ABSTRACT

Severe Plastic Deformation (SPD), applying extreme force to alterate and refine the structures of materials permanently, have a huge potential to improve the mechanical and structural properties of materials superiously. ECAP is a kind of SPD techniques to produce submicron or nano sized grains in the material structure by applying stress to the sample passing through two angular intersected channels have the same diameters. ECAP has recently been becoming one of the most favourable candidate method in the production of nanostructured materials.

One of the main objectives of this study and relating experiment is trying to understand how the properties of the material enhance under applied progressive and severe pressure. This process is directly related to the internal structure and texture of the material. A more strengthened material structure with superior properties is always desired to achieve. The material strengthening mechanism has been explained by dislocation theory which is based on the restricting the movement of dislocations through the crystalline lattice.

In this study, it is aimed to observe the reforms in microstructural and mechanical properties of aluminum alloys as a result of obtaining them in micro/nano grained structures by using ECAP technique. Consecutive experiments have been carried out in the Mechanical Engineering Laboratory of İzmir Katip Çelebi University. The rods with a diameter of 12 mm and a length of 30 mm were used as sample billets, which were not subjected to any heat treatment previously. A 120 ton capacity hydraulic press with pressing speed of 2mm/s and a sensitively machined die with channels of 120° intersected ($\Phi=120°$, $\psi=20°$) have been used. All the ECAP experiments in this investigation have been carried out at 120°C temperature condition. Prior to each repeating the process, the specimen was rotated using type of B_C route. Then, the analyses on ECAP applied samples were performed and the changes in crystal structure, microstructural and mechanical properties were investigated.

Changes in the crystal grain orientations of ECAPed samples were observed. At the same time, the grain size in the microstructure decreased by ECAP process. Furthermore, significant increase in microhardness values was determined.

EŞ KANAL AÇILI PRESLEME (EKAP) YÖNTEMİYLE ALUMİNYUM ALAŞIMLARININ MİKROYAPI VE MEKANİK ÖZELLİKLERİNİN GELİŞTİRİLMESİ

ÖZET

Yoğun bir şekilde kuvvet uygulanarak malzemelerin yapısını kalıcı halde değiştirip iyileştiren Aşırı Plastik Deformasyon (APD) yöntemi, malzemelerin mekanik ve yapısal özelliklerini mükemmel derecede geliştirmesi açısından güçlü bir potansiyele sahiptir. APD yöntemlerinden biri olan Eş Kanallı Açısal Presleme (EKAP) tekniği de aynı çaplara sahip açısal olarak kesişen iki kanaldan stres uygulanarak numunenin geçirilmesi sonucu malzeme yapısında mikronaltı veya nano ölçekte taneciklerin oluşumunu sağlar. EKAP, son zamanlarda nano yapılı malzemelerin üretiminde favori aday yöntemlerden biri haline gelmiştir.

Bu araştırmanın ve ilgili deneyin ana hedeflerinden biri, malzemenin özelliklerinin uygulanan progresif ve şiddetli basınç altında nasıl gelişim gösterdiğini anlamaya çalışmaktır. Bu süreç doğrudan malzemenin iç yapısı ve dokusu ile ilgilidir. Üstün özelliklere sahip daha sağlam bir malzeme yapısının elde edilmesi her zaman amaçlanmıştır. Malzeme mukavemeti, dislokasyonların kristal kafes boyunca hareketini kısıtlamaya dayanan teori ile açıklanır.

Bu çalışmada, Eş Kanallı Açısal Presleme (EKAP) tekniği kullanılarak mikro/nano tanecikli yapı elde edilmiesi hedeflenmiş ve metallerin mikroyapısal ile mekanik özelliklerindeki değişikliklerin incelenmesi yapılmıştır. Bu amaçla İzmir Katip Çelebi Üniversitesi Makine Mühendisliği Laboratuvarında ardışık bir dizi EKAP deneyleri gerçekleştirilmiştir. Daha önce herhangi bir ısıl işleme tabi tutulmayan 12 mm çap ve 30 mm uzunluğa sahip olan çubuklar, numune kütükleri olarak kullanıldı. 2mm/s hızında 120 ton kapasiteli bir hidrolik pres ve hassas bir şekilde işlenmiş 120°'lik kesişen kanalları olan kalıp ($\Phi = 120°$, $\psi = 20°$) kullanılmıştır. Bu araştırmadaki tüm EKAP deneyleri 120°C sıcaklık koşullarında gerçekleştirilmiştir. İşlemin her tekrarlanmasından önce örnek, B_C rotası kullanılarak döndürülmüştür. Daha sonra EKAP uygulanan numuneler üzerinde analiz yapılmış ve kristal yapıdaki değişiklikler ile mikroyapısal ve mekanik özellikler incelenmiştir.

EKAP uygulanan örneklerin kristal tane yönlerinde değişikliklerin meydana geldiği gözlemlenmiştir. Aynı zamanda mikroyapıdaki tane ebatları ECAP sonucunda küçülmüş olup ayrıca mikro sertlik değerlerinde de belirgin artışlar meydana geldiği tespit edilmiştir.

1. INTRODUCTION

Throughout the history of mankind there have always been efforts to acquire superior metallic or non-metallic elements. With the development of technology, investigations at nano-scale levels in materials engineering has recently become a favorite field. Metallurgical structures and mechanical properties of materials have a remarkable relationship between each others. Such processes known as Severe Plastic Deformation (SPD) applying excess force to alter and refine the structures of materials plastically have the potential to improve the mechanical and structural properties of the materials superiously. SPD techniques such as rolling, drawing, extrusion that widely preferred for strengthening metals, alloys or composites have been used in industrial applications for many years.

ECAP is a kind of SPD techniques which produces submicron or nano sized grains by applying stress to the sample passing through two angular intersected channels having the same diameters. While the specimen is passing from the first channel to the second, curling at a sharp corner, it's exposed a large amount of shear strain resulting with the deformation and grain refinement. The cross sectional dimensions of the specimen remains the same as the origin after each passes. Using this method keeps the waste of the material at minimum level. Then the process is repeated with the same specimen up to achieve a nearly perfect microstructure or even nanostructure. Moreover the texture and new structure of the specimen refined homogenously and resulting with enhanced mechanical properties. On the other hand, this technique has the potential to make a leap for nano engineering inventions. ECAP has recently been one of the most favourable method in the production of nano structured bulk materials [1].

Due to their convenience and vast range of simple or sophisticated industrial applications such as in automotive and aircraft productions we preferred to use Al and its alloys in this study (Figure 1.1) . Al7075 alloy is a non-corrosive alloy as it's used in automotive applications, gears and shafts, regulating valve parts, worm gears,

keys, fuse parts, aerospace and defense applications, bike frames, all terrain vehicle sprockets [2].
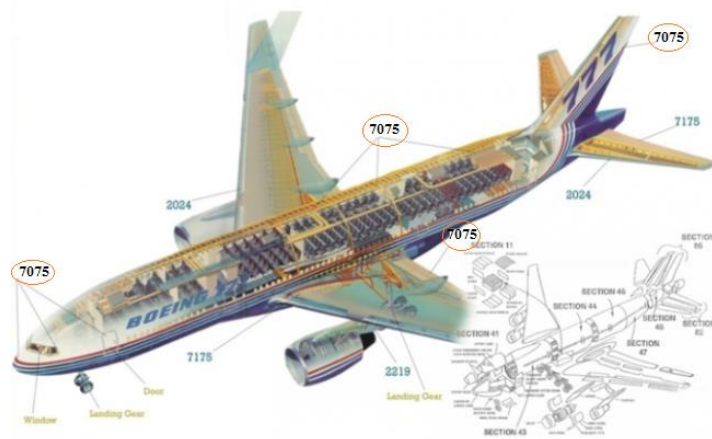
Figure 1.1 : Use of Al7075 in aircraft applications [3].

The products provided by ECAP procedure with superior mechanical, electrical or constructional properties can be in bulk rods, sheets or even in wire forms. This method is feasible in combining with many metal forming processes, thermomechanical treatments as well SPD techniques. It has been observed a considerable increase in mechanical properties such as values of strength obtained with supporting subsequent thermomechanical treatments. ECAP processed Ti–6%Al–4%V alloy has been given a succesful performance in dental applications and many other engineering products, for example, weight-sensitive products and special automotive components [1]. ECAP was first applied and developed by Segal and his colleagues at the Minsk Institute of the Soviet Union in the 1970s and 1980s. Despite the fact that it does not have the place in commercial area and industrial applications as it deserves, in terms of outstanding material features, this issue has attracted by plenty of material researchers [4].

This study consists of five chapters. After introduction, the fundamental terms and mechanisms of severe plastic deformation are described. The main characteristics of ECAP also explained in the same context. In the third chapter the materials and methodolgy used in the experimental setup presented, and in the fourth chapter the results of the experiments are discussed. Finally, in the last chapter the overall conclusions and important points of the study are pointed.

2. FUNDAMENTAL TERMS AND CONCEPTS

2.1 Material Strengthening

One of the main objectives of this research and relating experiment is trying to understand how the properties of material enhance under applied progressive and severe pressure. This process is directly related to the internal structure and texture of the material. A more strengthened material structure with superior properties is desired to achieve. The material strengthening has been explained by dislocation theory which based on the restricting the movement of dislocations through the crystalline lattice. Impurities, defects, vacancies and self-interstitials drive deviations from crystalline perfection of materials (Figure 2.1) .
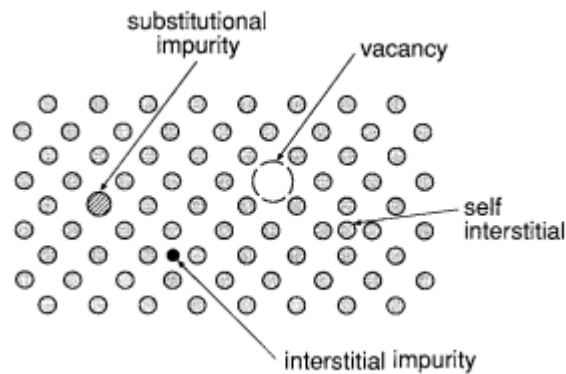
Figure 2.1 : Point defects in a crystalline solid [5].

That means there is no excellence in the crystal structure of the material. Thanks to deviations from crystallographic structure it's possible to process the metals for usage. Otherswise it would be needed huge forces and strains for deformation and refinement. Following plastic deformation, dislocations are piled up and absorbed by the subgrain boundaries. The strength (resistance to deformation) can be improved by putting obstacles to slip. Generally with increasing the hardness, ductility and toughness decrease and hence the plasticity of the material sacrificed to achieve a higher yield strength. Severe Plastic Deformation (SPD) strengthening forms an important topic in Materials Science field. There are numerous strengthening methods aimed to improve structural and mechanical properties such as grain boundary strengthening, cold working, martensitic strengthening, strain hardening, fibre strengthening, fine-particle strengthening, solid-solution strengthening and

strain ageing have been used [7, 8]. Even if it is not at the required place in production processes, ECAP is a candidate to be the most favourable SPD method in the last periods.

Dislocation propagations have been impeded with refining the grains in the internal structure of the material. The adjacent grains interact each other and due to the lattice structure they prevent each other to move in a continuous slip [5].

2.2 SPD Mechanisms

The main purpose of SPD is to refine the grained microstructure by applying excess force deforming the material irreversibly and as a result, mechanical and functional properties improved. Ability to deform plastically depends on the ability of dislocations to move (Figure 2.2) . Motion of a large number of dislocations happens during plastic deformation as well as the amount of dislocations increases extremely [6].
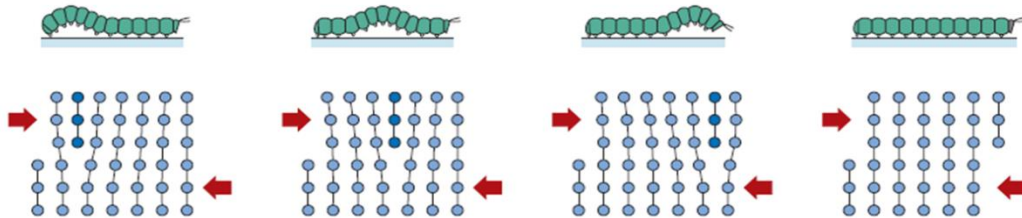
Figure 2.2 : The analogy between caterpillar and dislocation motion [6].

Plenty of SPD techniques have been applied in a vast range during historical old ages. Some have been applied in their own terms, but sometimes more than one technique has been used in the same application. The metal subjected to a hidrostatic pressure with imposing a very huge strain and the micro structure of the material was tried to be improved keeping the dimensions of the metal. The metal reforming procedure ends with structural regularities and changes irreversibly. The internal grains of the subjected material divide into subgrains up to micro or nano sizes which have small angle boundaries embeding the impurities and dislocations (Figure 2.3) .

As a result the mechanical, chemical, texture, micro structure and functional properties of the metallic materials enhance [7, 8].

Process	Schematic illustration	Equivalent strain
Basic processes (a) Equal-channel angular pressing (ECAP)		$\varepsilon_{eff} = N \frac{2}{\sqrt{3}} \cot(\phi)$ N, the number of ECAP passes
(b) High-pressure torsion (HPT)		$\varepsilon_{eff} = N \frac{2}{\sqrt{3}} \frac{\pi r}{t}$ r, the distance from the axis, t, the thickness of the sample, N, the number of revolutions
(c) Accumulative roll bonding (ARB)		$\varepsilon_{eff} = N \frac{2}{\sqrt{3}} \ln(\frac{t_0}{t})$ t_0, the initial thickness of the sample, t, the thickness of the sample after rolling, N, the number of passes
(d) Multi-axial forging		$\varepsilon_{eff} = N \frac{2}{\sqrt{3}} \ln(\frac{a}{b})$ Strain is non-uniform. N, the number of processing steps
(e) Twist extrusion (TE)		$\varepsilon_{eff}^{min} \approx 0.4 + 0.1 \tan\gamma$; $\varepsilon_{eff}^{max} \approx N \frac{2}{\sqrt{3}} \tan\gamma$ γ is the twist line slope; N is the number of passes. Deformation is non-uniform
Derivative processes (f) Repetitive side extrusion		ECAP equivalent

Figure 2.3 : Schematic illustration of traditional and novel SPD methods [8] *(to be continued).*

(g) Rotary-die ECAP
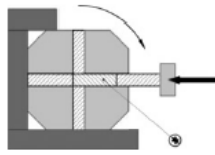
ECAP equivalent

(h) Cyclic extrusion–compression (CEC)
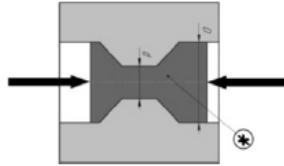
$\varepsilon_{eff} = N4\ln\left(\frac{D}{d}\right)$
N, number of cycles

(i) Cyclic close-die forging (CCDF)
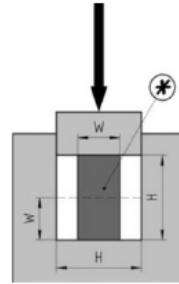
$\varepsilon_{eff} = N\frac{2}{\sqrt{3}}\ln\left(\frac{H}{W}\right)$
N, number of cycles

(k) Repetitive corrugation and straightening (RCS)
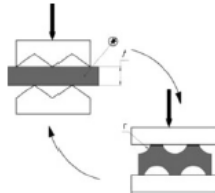
$\varepsilon_{eff} = N\frac{4}{\sqrt{3}}\ln\left(\frac{r+t}{r+0.5t}\right)$
N, number of cycles

Integrated processes
(l) Integrated extrusion + ECAP
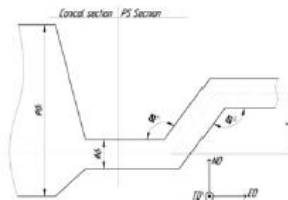
(m) Parallel channel ECAP (PC-ECAP)
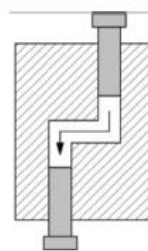
ECAP equivalent

Continuous processes
(n) ECAP- Conform
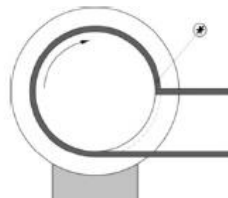
Figure 2.3 : Schematic illustration of traditional and novel SPD methods [8] *(to be continued).*

(o) Con-shearing
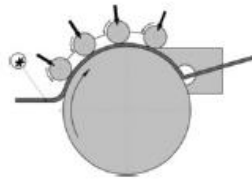
(p) Continuous confined strip
    shearing (C2S2)
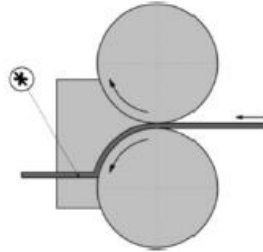
(q) Continuous repetitive corrugating
    and straightening (RCS)
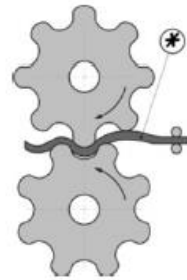
(r) Incremental ECAP (I-ECAP)
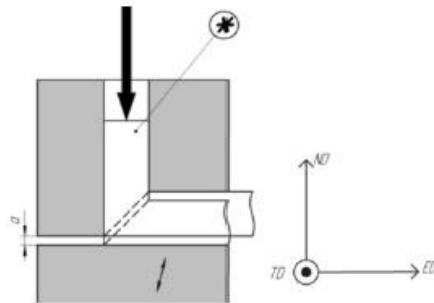
(s) Continuous high-pressure torsion
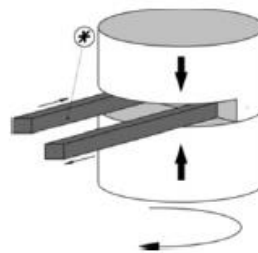
(t) Continuous manufacturing
    of bolts
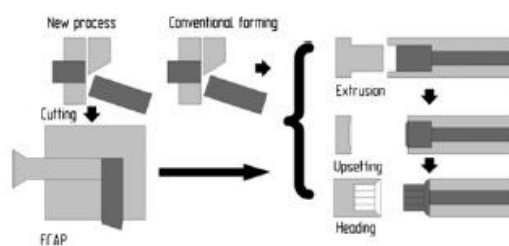
Figure 2.3 : Schematic illustration of traditional and novel SPD methods [8].

There are many types of SPD techniques. ECAP also have different kinds in terms of die design (Figure 2.3) . Among all of these, high-pressure torsion (HPT) and ECAP are the most ambitious and commonly used techniques in order to refine the microstructure resulting with improving material properties [8,9,10].

2.3 Strengthening by Grain Refinement

The finer the grains means the larger the area of grain boundaries with lower angles that impedes dislocation motion.

The yield strength (σ_y) is expected to vary with grain size d according to Hall-Petch relationship (equation 1):

$$\sigma_y = \sigma_0 + k_y / d^{1/2} \tag{1}$$

where σ_0 is the lattice friction stress, and k_y is a constant of yielding.

S. Han et al studied on 99.99 % pure, oxygen-free copper processed by ECAP [11]. Because of the strain hardening in the initial stage, the increasing in the values of yield and tensile strength observed. But in the advanced pass numbers, equiaxed grains formation occurs and the dislocation density decreases at the same time. This phenomenon is also accelerated by the extremely high rate of dynamic recovery with the grain boundary area. As a result the hardening progress stops and the fine grain boundary hardening mechanism propagates following the fourth pass. The size of that equiaxed grains did not vary up to further eight passes while the dislocation density inside the grains decrease (Figure 2.4) . So the ductility values increase and the strength stays in nearly constant values from four to eight passes [11]. Similar consequences have been reported also for Al alloys [12].
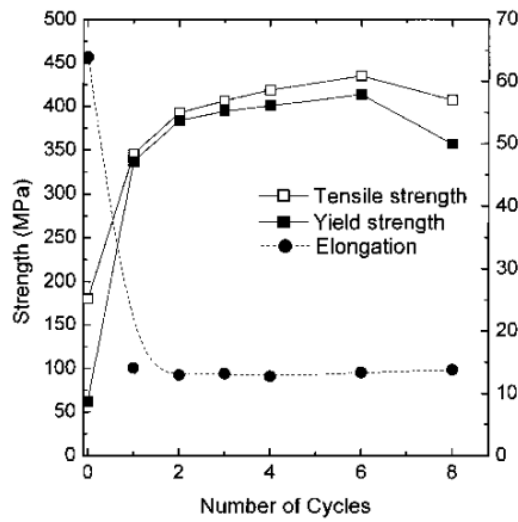
Figure 2.4 : Change in tensile values with respect to ECAP passes(cycles) [11].

The experiment results show that Hall-Petch equation does not satisfy enough in explaining the trend of yield strength (Figure 2.5) .
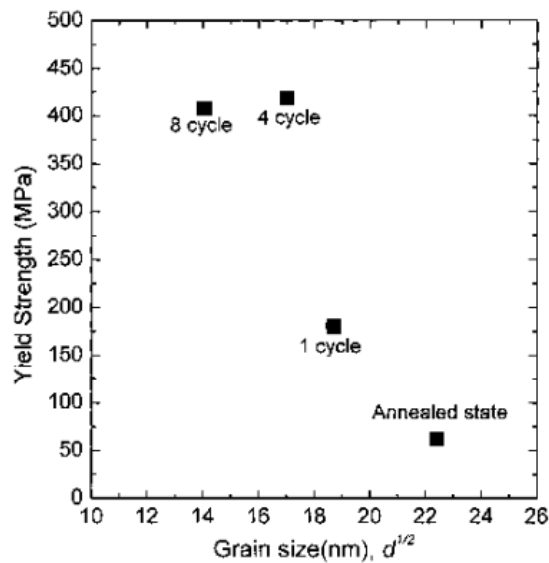
Figure 2.5 : Hall–Petch relationship at different numbers of passes(cycles) [11].

In the following periods, the issue have been needed new models (Table 2.1) also including the strain hardening mechanism, grain boundary crystallography, thermodynamics of interface structure and the fine grain boundary hardening mechanism as well as dynamic recovery [13].

Table 2.1 : Summary of grain size strengthening models [13].

Model		Year	Equation	Physics
Pile-up	Hall Petch	1951 1953	$\sigma_y = \sigma_0 + k \dfrac{1}{\sqrt{D}}$	Grain boundaries (GBs) are obstacles preventing dislocation motion. Dislocations emit into adjacent grains when the shear stress at the head of a dislocation pile-up reaches some threshold value.
	Cottrell	1958	$\sigma = \sigma_0 + \tau_d \sqrt{\dfrac{l}{D}}$ l = distance from GB to source τ_d = unpinning stress	Stresses generated by dislocation pile-ups in one grain activate Frank-Read sources in adjacent grains.
	Armstrong et al.	1962	$\sigma = \sigma_0 + \tau_d m^2 \sqrt{\dfrac{l}{D}}$ m = Taylor orientation factor	Similar model to Cottrell's but accounts for the fact that the dislocation source might be on a different slip system than that of the dislocation pile-up. Accounts for the effect of crystal structure on k through the Taylor factor, m.
	Navarro and de los Rios	1988	$\sigma = \sigma_0 + \dfrac{2\tau_d m^2}{\pi} \sqrt{\dfrac{l'}{D}}$ l' = "effective position" of source	Similar model to Cottrell's but the dislocation source is assumed to extend over a finite distance.
	Friedman and Chrzan	1998	$\sigma = \sigma_0 + \sqrt{\tau_d^2 + \dfrac{Gb\chi}{\pi D}}$ χ = constant	Similar to the Cottrell model but dislocations can exert backstresses that make it more difficult for Frank-Read sources to operate.
GB source	Li	1963	$\sigma = \sigma_0 + \alpha Gb \sqrt{\dfrac{3s}{D}}$ s = line length of dislocation α = constant of order unity	Dislocations generated from GBs at yielding strengthen the material through the Taylor equation. The density of dislocations generated at yielding is proportional to the GB area because the dislocations are generated at GB ledges.
GND	Ashby	1970	$\sigma = \sigma_0 + CG \sqrt{\dfrac{b\varepsilon}{D}}$ C = material-dependent constant	Compatible deformation of individual grains in a polycrystal requires the introduction of geometrically necessary dislocations (GND's). Density of GND's is inversely proportional to the grain size. GND's affect the strength through the Taylor equation.
Composite	Thompson et al.	1973	$\sigma = \sigma_0 + \left(1 - \dfrac{\lambda_S}{D}\right)\left(\dfrac{K_1}{D}\right) + \dfrac{\lambda_S}{D}\sqrt{\dfrac{K_2}{D}}$ λ_S = statistical slip length K_1, K_2 = constants	Treat the individual grains as composites with different dislocation densities in the grain interior and the region near the grain boundary. Dislocations affect the strength through the Taylor equation.
Slip distance	Conrad	1963	$\sigma = \sigma_0 + \alpha G \sqrt{\dfrac{b\varepsilon}{\sqrt{D}}}$ ε = strain	Assumes that the grain size affects the dislocation density, which affects the strength through the Taylor equation; that dislocations are not annihilated during the early stages of plastic straining; and that the dislocation slip distance is proportional to square root of the grain size.
	Meakin and Petch	1974	$\sigma = \sigma_0 + \theta m^2 G\varepsilon + \tau_d m^2 \sqrt{\dfrac{l}{D}} + \alpha m^{3/2} G \sqrt{\dfrac{b\varepsilon}{D}}$ θ = material-dependent constant	Combines the traditional pile-up model with the slip distance model due to Conrad.

ECAP process has a great potential to reduce the size of grains into nano levels. There have been many efforts to show the relationships between the grain size and the strengthening mechanism. But, due to complexity of the gain refinement growth such as rotations, shear band formations, dislocation-grain boundary interactions some deviations have been reported. The strain rate, the temperature, dislocation interactions, grain-boundary sliding and grain size dispersion are intensively need to be considered. Furthermore for most of metals, at the ranges above about 10 nm diameters of grains, the indepence and deviation from Hall-Patch formula prevailing. It can be concluded that, for coarse-grain polycrystalline materials up to a critical point which about 10 nm (Figure 2.6) , the strength increase with decreasing grain size [14-21].
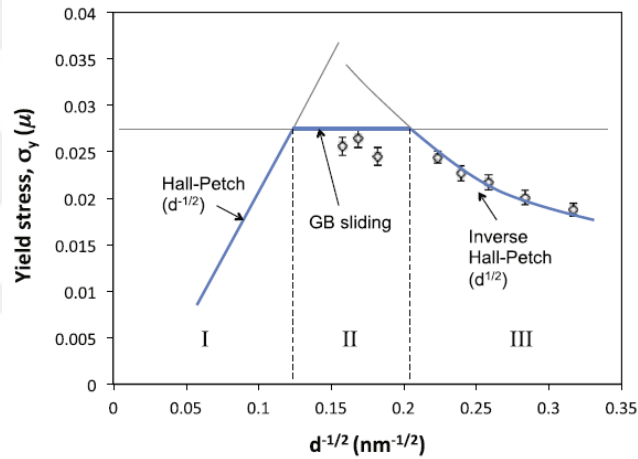
Figure 2.6 : Different regimes of grain size effect on yield stress. Regime I is the classical Hall–Petch regime dominated by dislocation pile-up against GBs. Regime III is the inverse Hall–Petch regime dominated by lattice dislocation emission from triple junctions as a result of GB sliding. And an intermediate regime II where pure GB sliding dominates [21].

2.4 Properties of Ultra-Fine Grained (UFG) Materials Produced by ECAP

The nanomechanics of the materials has been becoming one of the most interesting scientific as well as industrial field in parallel with the technological development. The material structure has been classified according to its grain size from conventional to atomic level (Figure 2.7) . Nowadays ECAP technique seems to be

successful in producing UFG structured bulk materials with applying severe forces while passing through two intersected channels [22].
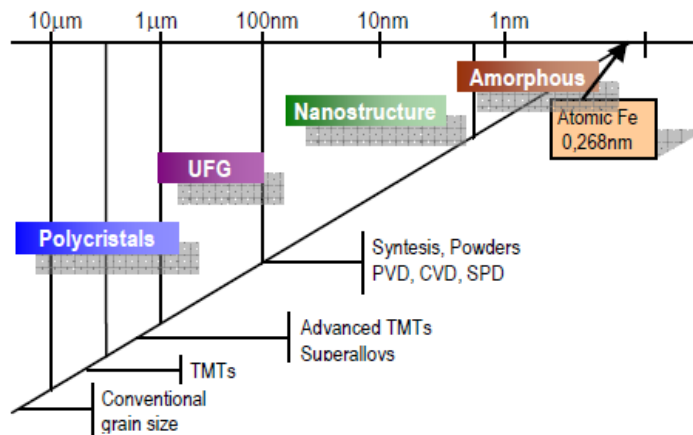
Figure 2.7 : Schematic illustration for grain size refinement [22].

Plenty of investigations have been done about the effects of ECAP on the nanostructural as well as mechanical properties of the metals, alloys and composites. The analysis of the characterization tests results are discussed in a comparative attitude to meet at the common denominators and prescriptions.

M.Furukawa et al conducted some experiments to search the principles of shear distributions and with sample rotations effects of ECAP process [23]. They showed geometrically the shearing strain imposed to the material and the directions of the shearing segments determined by the routes of the subjected sample before each pass (Figure 2.8, Figure 2.9) .
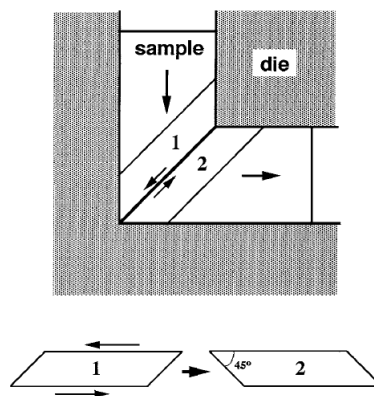
Figure 2.8 : The basic principle of shearing durimg ECAP [23].
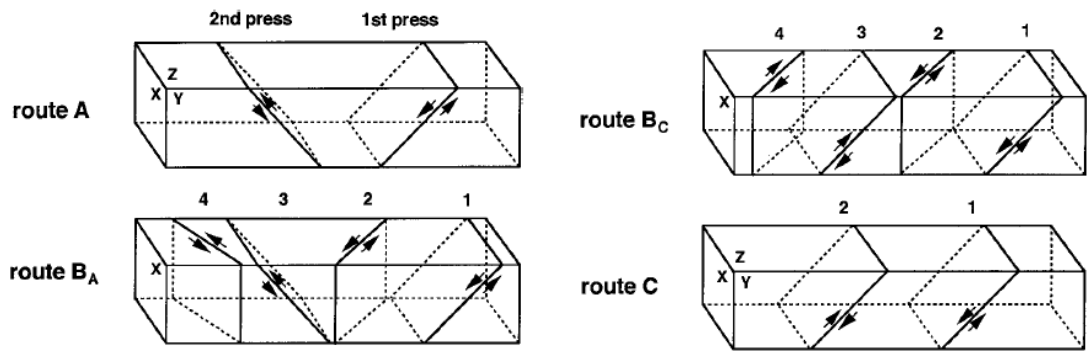
Figure 2.9 : The shearing planes concerning processing rotations [23].

S. M. Kumar et al pressed Al7075 billets through the channel with 90° die angles after annealing at 412 °C for 1 h and then cooled to room temperature. They have observed that the structure with grains of 400–440 nm achieved in route B_C after four passes [24].

M. Reddy et al studied on Al7075 alloy die angle 120° up to 3 passes and determined that ultimate tensile strenth increases from 329 MPa as received, reaches about 487 MPa after first pass. The hardness value is increased from 125 HV to 197 HV at the end of third pass [25].

M. Saravanan et al studied on pure aluminum with 90° die angles at room temperature up to eight passes and determined with AFM characterization as the grain sizes reduced from 150 μm to ~620 nm [26]. They have taken photomicrographs showing the grain alteration of raw material and pressed specimens up to fourth pass. Although the grain boundaries are not very clear, the grain dividing can be followed obviously (Figure 2.10) . They also showed the variation of hardness values with the pass numbers (Figure 2.11) . They predicated the low hardness values with decreasing in dislocation density and the formation of equiaxed grains in certain passing numbers. It has been also pointed that with increasing impurity content more pass numbers needed to achieve UFG and homogenious microstructure. Furthermore, the ultimate equilibrium grains become finer with decreasing purity [26].
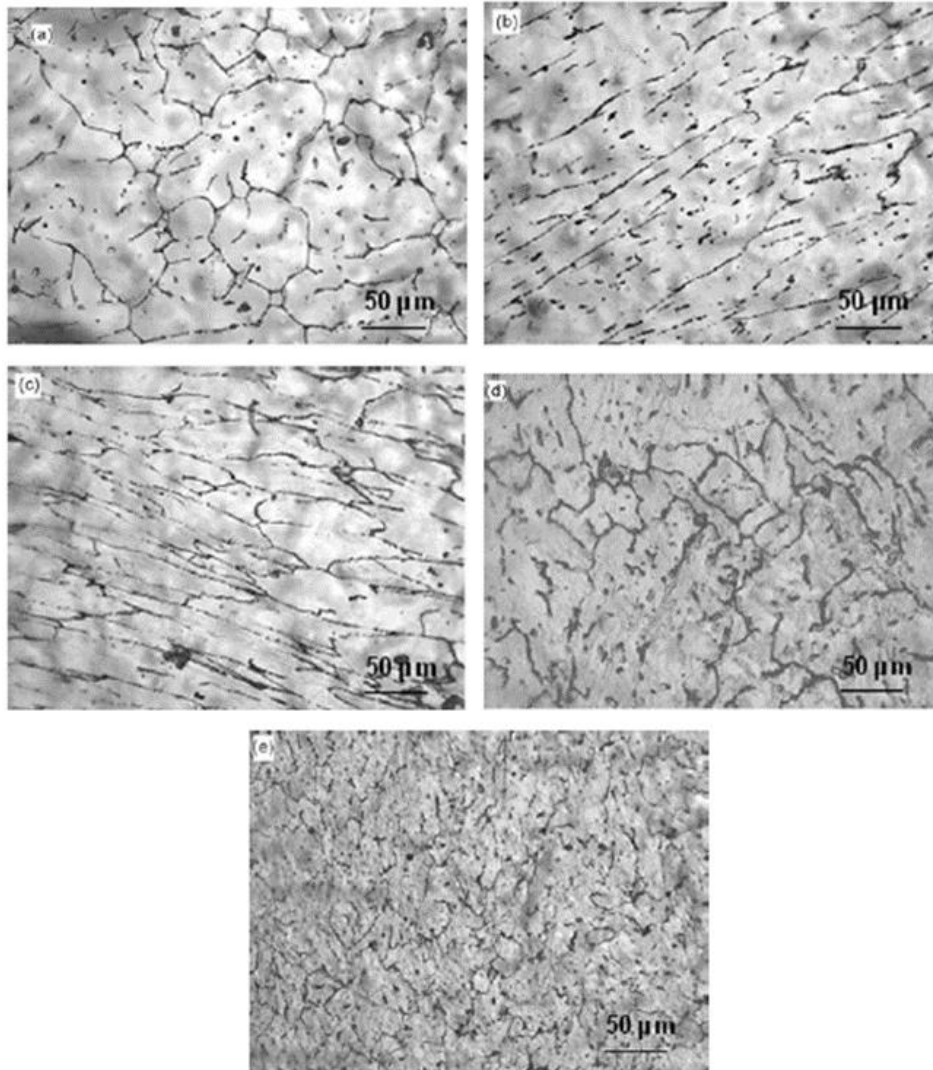
Figure 2.10 : Optical microstructures of 99.5% pure Al: (a) unpressed, (b) first pass, (c) second pass, (d) third pass and (e) fourth pass [26].
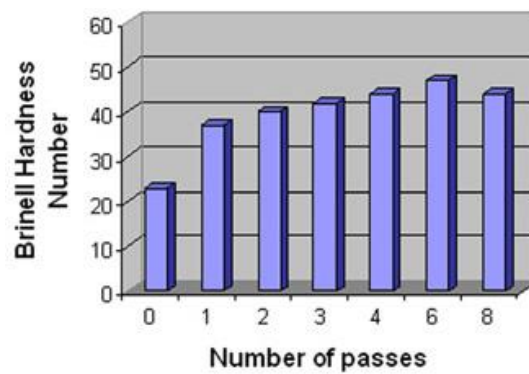
Figure 2.11 : Hardness values versus number of passes in 99.5% pure Al [26].

14

3. MATERIALS AND METHOD

3.1 Tested materials

Due to their commonly usage in the industrial application, commercial aluminum alloys such as pure Al (99,5% Al), Al7075 and Al6013 alloys were used in this study as experimental materials. Al7075 have been processed up to 10 passes in the experiment. The other two Al6013 and pure Al processed up to 4 passes. Al7075 alloy has been studied here as the main material. The other two alloys are studied as suplementary works. The chemical compositions and main mechanical properties of the aluminum alloys that supplied in the extruded rod from manufacturer are given in Table 3.1 and Table 3.2 respectively. All the samples have been supplied from the metal market and have been commonly using in industrial applications. Then the rods have been machined in the intended sizes as sample billets compatible with die design.

Table 3.1 : Chemical compositions of aluminum alloys used in this study [27-29].

Elements	Pure Al	Al 7075	Al 6013
Al	99.5	87.1-91.4	94.8-97.8
Fe	0.4	0.5	≤ 0.50
Si	0.1	0.5	0.60-1.0
Cu	0.05	1.2-2.0	0.60-1.1
Mn	0.01	0.3	0.20-0.80
Mg	0.05	2.1-2.9	0.80-1.2
Zn	0.07	5.1-6.1	≤ 0.25
Cr	0.01	0.18-0.28	≤ 0.10
Zi+Ti	0.05	0.25	≤ 0.10
Others	0.03	0.15	≤ 0.050

The aluminum alloy bars further machined to the billets form of Ø12 mm diameter and 30 mm in length. All the samples used here have the same dimensions and not subjected to any heat treatment before installing the die. All the ECAP experiments in this study have been carried out at 120°C temperature condition by heating the die with probes.

Table 3.2 : Mechanical properties of the aluminum alloys [27-29].

Properties	Pure Al	Al 7075	Al 6013
Yield Strength (MPa) min-max	20-35 *(0)* 90-105 *(HX4)* 110-140 *(HX8)*	105 *(T0)* 460-505 *(T3)* 435 *(T6)*	170 *(T0)* 317 *(T6)* 379 *(T8)*
Tensile Strength (MPa) min-max	65-80 *(0)* 110-115 *(HX4)* 130-150 *(HX8)*	225 *(T0)* 530-570 *(T3)* 505 *(T6)*	310 *(T0)* 359 *(T6)* 392 *(T8)*
Elongation (%50) min-max	38 *(0)* 9 *(HX4)* 5 *(HX8)*	17 *(T0)* 10 *(T3)* 12 *(T6)*	22 *(T0)* 8 *(T6)* 5 *(T8)*
Hardness (brinell) min-max	20-21 *(0)* 35-36 *(HX4)* 43 *(HX8)*	60 *(T0)* 140-160 *(T3)* 140 *(T6)*	60 *(T0)* 140 *(T6)* 130 *(T8)*

After placed in the die centered, with starting the pressing machine load applied from entry channel and flow through the next 120° intersected channel without any change in the diameter, and in the weight of the billet. Even though the sample processed in ECAP can be in cylindirical, rectangular, sheet, plate or any other similar shape our tests were conducted using cylindrical ignot billets [30].

3.2 ECAP Procedure and the main parameters

Some consecutive ECAP experiments have been carried out in the Mechanical Laboratory of İzmir Katip Çelebi University subsequently using a universal hydraulic press equipment with a capacity of 120 ton and related setup tools.

Hydraulic Press, ECAP die and billet samples are the main components of the ECAP process. Before starting the experiment these three components need to be designed and prepared meticulously. Otherwise, blockage of the sample and punch damages are inevitable. Throughout plenty of ECAP trials and observations we have determined the following main important parameters that must be watch out carefully:

- Controllable pressing unit to fulfill required pressure.

- The material sample with proper size for ECAP process.

- ECAP die material and design [30].

- Intersection angles of die channels. The optimum strain homogeneity can be achieved with $\varphi = 90°$, $\psi = 15°$ [36].

- Surface quality of the channels [31].

- Pressing speed. Optimum: 2mm/sec [31].

- Plunger to push the samples; must be chosen with proper material, surface quality and dimensions to prevent buckling and seizing [31].

- Lubrication agent applying to the sample and to the die channels [34].

- Heating the billet sample. The increase of pressing temperature in the production of ultra fine grained materials facilitates the process, while the grain size also affects the negative direction and causes the grain size to increase [32].

- The number of passes repeating up to achieve a homogeneous microstructure [26].

- Rotating the sample around its axis at specified routes prior to each repeating the process [37].

Even though there is a wide range of experimental factors that influence in achievement of advanced microstructural and mechanical properties, the most important key parameters are channels geometry, contact friction and tool design [33].

3.2.1 Hydraulic Press Machine

In this experiment, specimens were pressed approximately at 80 tones even though the press capacity is 120 tones. The speed of the press designed to be min. 1 mm/sec and max. 4 mm/sec. The optimum speed used here: 2 mm/sec. Transparent safety cover to ensure work safety while in operation (safety first!).

Experimental equipment includes a hydraulic press with maximum load of 120 ton, supplied from Turkyus Laboratory Technologies (Figure 3.1) .

Figure 3.1 : Overall view of hydrostatic pressing machine installed in the Mechanical Engineering Laboratory of İzmir Katip Çelebi University.

It is constructed on four 80 mm diameter induction Cr-coated columns having vertical axis. This press is designed and built with a hydraulic drive unit and tool mountable table being moved vertically by the hydraulic cylinder, primarily considering ECAP process applications. Both the fixed and the moving table are manufactured from ST52 quality filled Platinum material. Both bottom and top tables have slots to fix ECAP die and plunger with its mandrel. There is an electric panel which command any pressing movement. Controlling the up and down movement takes place with the electric buttons. The gap between lower fixed table and movable table is maximum 700 mm. Pressing moving table is bedded with bronze bushes. The 4200 watt external heating unit with electronic display and 6 heating resistance are ready for use. There is a transparent safety cover to ensure work safety while in operation. The speed is adjustable and the pressure can be controlled during operation. The speed of the press designed to be min. 1 mm/sec and max. 4 mm/sec. As a result of various trials, we noticed that 2 m/s speed could be optimum for ECAP and we continued our work in this manner. Specimens were forced approximately at 80 tones that fulfill passing Al alloys through the channels during the pressing regimes.

3.2.2 ECAP Die Block

Two machined channels have the same diameters as Ø12 mm and intersecting 120 degrees. Pressing temperature depends mostly on the type of billet material. For materials of low ductility more heating of the die is necessary.

It is made from AISI H13 DIN 1.2344 steel and have a steel block surrounded and a mountage basement. There are holes through the steel block to put heatig cartridges. The die of ECAP cosists of two symmetrical half parts, machined from two blocks of steel and heat treated to achieve a nominal hardness of 62 HRC. Two machined channels have the same diameter as Ø12 mm and intersecting 120 degrees (Figure 3.2) . These two equal cross sectioned channels were machined with outer and inner radius transition (R: 4 mm and r: 2 mm, respectively) between the two channels intersecting at 120° (Figure 3.2) .
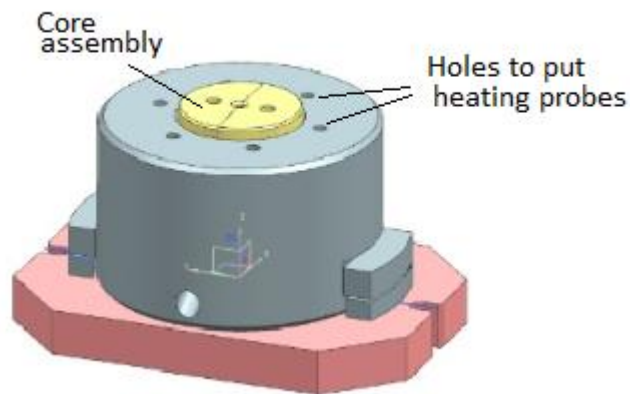
Figure 3.2 : ECAP Die geometry and 120° intersected channels.

3.2.3 Lubrication Agent

The mold inner surfaces and the billet specimen must lubricated plenty and uniformly to reduce the friction and abrasion as much as possible. It is important with respect to reduce and control bad frictional effects, produce more strain homogenous parts, prevent die failures, and decrease press tonnage in ECAP process. Thanks to suitable lubrication with making an oil film, the specimen slides easily and any damage can be prevented. So the high surface quality during sliding will be acquired and the grain refinement will be more homogenized. It is revealed that, determining the appropriate lubricant type and meticulous lubrication during ECAP cycles play a very essential role to achieve the expected targets. Especially in the stage of scale-up the ECAP processing tools for industrial applications and commercialisation, lubricant types should have been tested with all respects and optimized [34].

In this study, a graphite containing oil based lubricant, DIE FORGENT WLA 245 (obtained from Petrofer Industrial Oils and Chemicals, İzmir, Turkey) was applied to the mold inner surfaces and the sample to reduce friction and abrasion (Figure 3.3) . As can be seen from the manufacturer website the properties of this Forging Lubricant are as follows: Water-miscible and oil based lubricants for hot forging, die-forging and hot pressing. Also suitable as the die lubricant for circulation-systems on automatic forging machines [35].

Figure 3.3 : Graphite based oil.

3.2.4 Route types

Every of these routes are related to different slip system and strain value happen in the ECAPed material. To achieve the requested homogenious UFG microstructure, the rod must be rotated orderly prior to every putting in the die channel for pressing.

Different route types can be applied in ECAP processing. It is based on the principle of rotating the sample around its axis at different angles just before each passing procedure [37].

If the sample is not rotated about its own axis (0°) for each pass, this is the route A.

Route B_A is the method of rotating the sample around its own axis by ±90° continuously as the sample is at +90° in the first pass and then -90° in the next pass. It's named as the Route B_C if the sample is continuously rotated +90° on each pass. On Route C, the material is rotated 180° in each pass around its axis (Figure 3.4) .
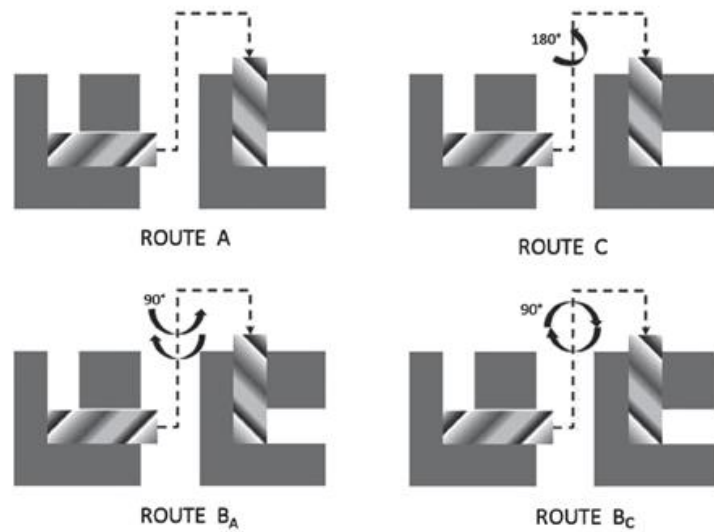
Figure 3.4 : The main processing routes of ECAP [37].

B_C is the optimum route in which microstructural evolution occurs mostly [38,39]. Two process parameters, repeating the passes and following up the proper billet orientation, produce large cumulative shear strain and various slip planes directions. Hereby, a homogenized microstructure is obtained [40].

Using Route B_C, it was carried out under a pressure of 80 tons and a pressing speed of 2 mm/s in the present study.

3.3 Methodology of Metallographic Sample Preparation

A systematic method has been followed to examine the microstructures of the materials during the sample preparation process of this study. The aluminum samples with and without ECAPed were prepared for microstructural and microhardness investigations with the metallographic sample preparation treatments. Due to the size limitation for the inspection with optical microscobe or any other device, samples need to be cut out with sensitive cutting machine. It was aimed to determine the most intense ECAP effects on the material by taking samples from the center of the billet specimens.

30 mm long specimens were cut from a 12 mm diameter Al7075 round section bar and made ready for ECAP processing. For Al7075 alloy from 1 to 10 passes were performed succesfully after many failures (Figure 3.5) . For commercial pure aluminum and Al6013 alloy up to 4 passes have been done.

Figure 3.5 : Typical appearance of ECAPed sample billets of Al7075.

Following ECAP process, the specimens were cut out with a diamond saw by using a precision cutting device Struers Accutom-5 (Figure 3.6) in order to carry out characterization processes of 2 pieces, transverse and longitudinal from centre of unpassed and passed billets.

Figure 3.6 : Cutting Device.

After cutting and taking out the samples from the center of the billets, the laboratory hot-mounting press Struers Citopress-1 (Figure 3.7) has been used to take bakalite with thermoset polymer filler. So the samples were inserted into a regular form, handled easily by hand polishing or bonded to the automatic polishing device. The sample is buried in thermoset or thermoplastic polymers at high temperature and pressure.

Figure 3.7 : Laboratory hot-mounting press.

To study the effect of severe plastic deformation on billets, each passed one is cut in two precisions along the x-axis and the y-axis as two separate samples.

Phenolic based conductive resin containing carbon filler has been used to prepare an ideal mold for characterization analysis and excellent edge sharpness. Each 3 cm diameter bakalite part is ready after heating and cooling the filler under pressure in 5 minutes (Figure 3.8) .

Figure 3.8 : Samples after bakalite mounting.

Mechanical sample holder grinding and polishing machine rotating in its own axis has been used after bakalite process (Figure 3.9) .

Figure 3.9 : Automatic grinding and polishing machine.

Some of the samples grinded and polished using conventional machine holding by hand during operation (Figure 3.10).

Figure 3.10 : Manual grinding and polishing machine.

Following bakalite procedure the moulded samples have been grinded with SiC coated sandpapers up to 2000 grit. Abrasive paper series such as 240, 400, 600, 800, 1200, 1500, 2000 grit are followed from the coarse to the fine. During the grinding process, fine abrasion marks are formed on the surface to be removed in the next sanding step. At the end of the grinding, if there is any damage on the surface, this damage must be from the last grinding step. Such kind of damages are eliminated by the polishing stage. After achieving a finer grinding, polishing is carried out to obtain a flat surface free of scratches in mirror gloss. Polishing pads has been mounted to the manual machine and then 1μm diamond compound applied to the pad and so the final polishing has been done (Figure 3.11) .
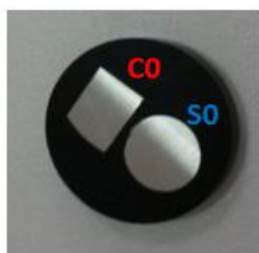
S0:	Unpresssed, cross section
C0:	Unpresssed, longitudinal section
S4:	4th pass, cross section
C4:	4th pass, longitudinal section

Figure 3.11 : Samples polished and get ready for characterization tests.

Finally, the samples were etched by Keller's solution such as included 2 ml HF, 3 ml HCl, 5 ml HNO3 90 ml water and get ready for optical microscope inspection and other characterization analyzes.

3.4 Characterization Methods

3.4.1 X-ray diffraction (XRD) analysis

The XRD analysis of "as received" and ECAPed samples were performed by Bruker D2 Phaser X-ray diffractometer with CuKα radiation (λ=1.5406 Å) at 30kV in the 0.02° intervals of 5–90°. In the present study, XRD analysis was performed to determine their phase content and to understand that how the crystalographic orientations of the grains changes after the ECAP process of the samples (Figure 3.12) .

Figure 3.12 : X-ray diffractometer (XRD) (Bruker D2 Phaser).

3.4.2 Microstructural analysis

The microstructural analysis, grain shapes and grain size measurements of as-received samples and ECAPed samples were analyzed by optical and scanning electron microscopy.

3.4.2.1 Optical microscopy

The microstructure of both "as received" and ECAPed samples were studied by Eclipse LV150N microscobe using digital imaging combined with advanced optical system (Figure 3.13) .

Figure 3.13 : Eclipse LV150N optical microscope.

3.4.2.2 Scanning Electron Microscopy (SEM) Analysis

The microstructure of both "as received" and ECAPed samples were studied by Quanta FEG 250 microscobe using high-resolution imaging of microstructure and composition analysis (Figure 3.14) . SEM images have been enabled by using the microscope installed at İzmir Institute of Technology Center for Materials Research (İYTE-MAM).

Figure 3.14 : Quanta FEG 250 SEM.

3.4.3 Mechanical properties

- Micro-vickers hardness tests. Based on the principle of creating a trace of a standardized pyramid-shaped diamond tip with a base square and a peak angle of 136°, immersed in the sample surface under variable loads. The test load applied here is HV 0,2 / 1,961 Kgf(N) for 10 sec. Five hardness values were measured from each sample to acquire more reliable results. The points selected randomly. Then the mean value and standard deviation calculated (Figure 3.15) .

Figure 3.15 : Shimadzu HVM Microhardness Tester.

- Nano-indentation techniques measure elastic modulus, hardness. Using a suitable indenter, a load is applied up to a maximum value determined to be perpendicular to the sample surface, and after this maximum load value is reached, it is reloaded gradually again. The mechanical properties of the specimen were determined by analyzing the Load (N) - Depth (nm) curves obtained as loading and reloading the results. In this study Nano-indentation tests applied to 4 specimens of Al7075 at 5 different loads (50, 100, 150, 200 and 250 mN).

4. RESULTS AND DISCUSSION

4.1 X-Ray Diffraction (XRD) Analysis of the Samples

It's revealed that ECAP process cause a considerable amount of distortion in the lattice structure of the deformed materials, since the peaks shift can be related to long range stresses as well as sub grain boundaries generated by deformation of crystallographic structure. Increase in dislocation density due to lattice microstrain and size effect can be correlated. Differences arise through the peak intensity and peak positions of the ECAP processed material. Following each pass, crystallographic structure orientations and crystal size changes have been happened (Figure 4.1) .
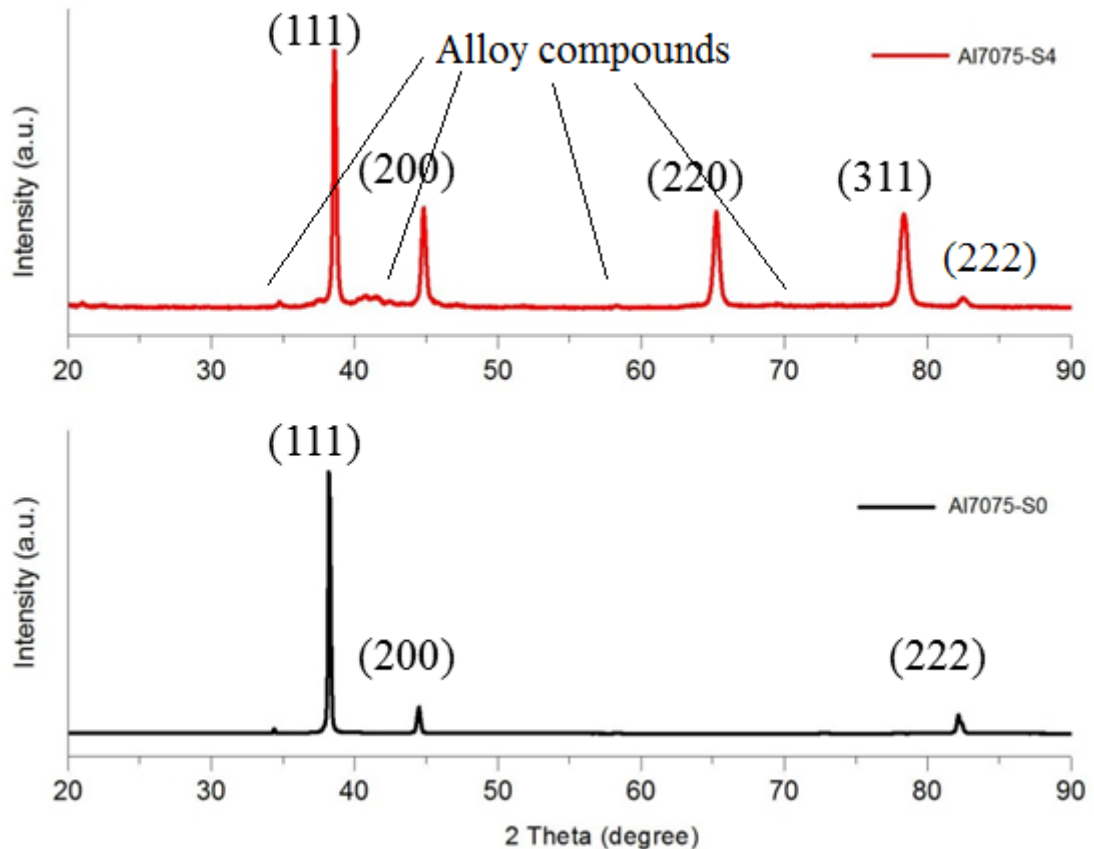
Figure 4.1 : XRD patterns of the Al7075 samples with four passes and no pass.

After obtaining data from XRD analysis the crystallite size of the ECAPed samples have been calculated by using Debye-Scherrer Equation.

Paul Scherrer (1918) first observed that small crystallite size could give rise to peak broadening [41]. He derived a well-known equation for relating the crystallite size to the peak width, which is called the Scherrer formula (equation 2):

$$t = K\lambda/(B \cos\theta) \qquad (2)$$

where

t is the averaged dimension of crystallites;

K is the Scherrer constant, somewhat arbitrary value that falls in the range 0.87-1.0 (it is usually assumed to be 1);

λ is the wavelength of X-ray; and

B is the integral breadth of a reflection (in radians 2θ) located at 2θ.

Calculations has done with Scherrer formula using data availed from our Al7075 cross sectional samples and a graph prepared accordingly (Figure 4.2) .
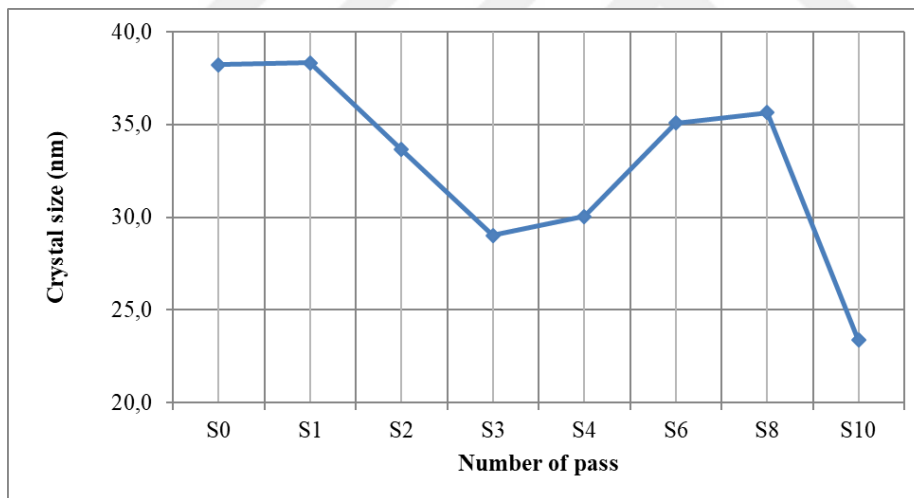
Figure 4.2 : Crystal size values of Al7075 samples (S direction) after ECAP calculated by Scherrer formula.

With respect to the graph, crystal sizes remained the same with the original sample at the first pass. From the first pass to third one there is a remarkable reduction in the crystal diameters as we can interpret it as a grain refinement happening. Recrystallization and dynamic recovery are propagating up to eighth pass and at tenth pass it can be said that the crystal division has a tendency to increase again while diameters are reducing up to achieve the final homogenous UFG refinement.

30

X-Ray Diffraction (XRD) analysis data of all ECAPed samples have been studied and can be seen in the following pages (Figure 4.3 - Figure 4.6) .

Figure 4.3 : XRD patterns of Al7075 samples in direction "S" after ECAP.

Figure 4.4 : XRD patterns of Al7075 samples in direction "C" after ECAP.
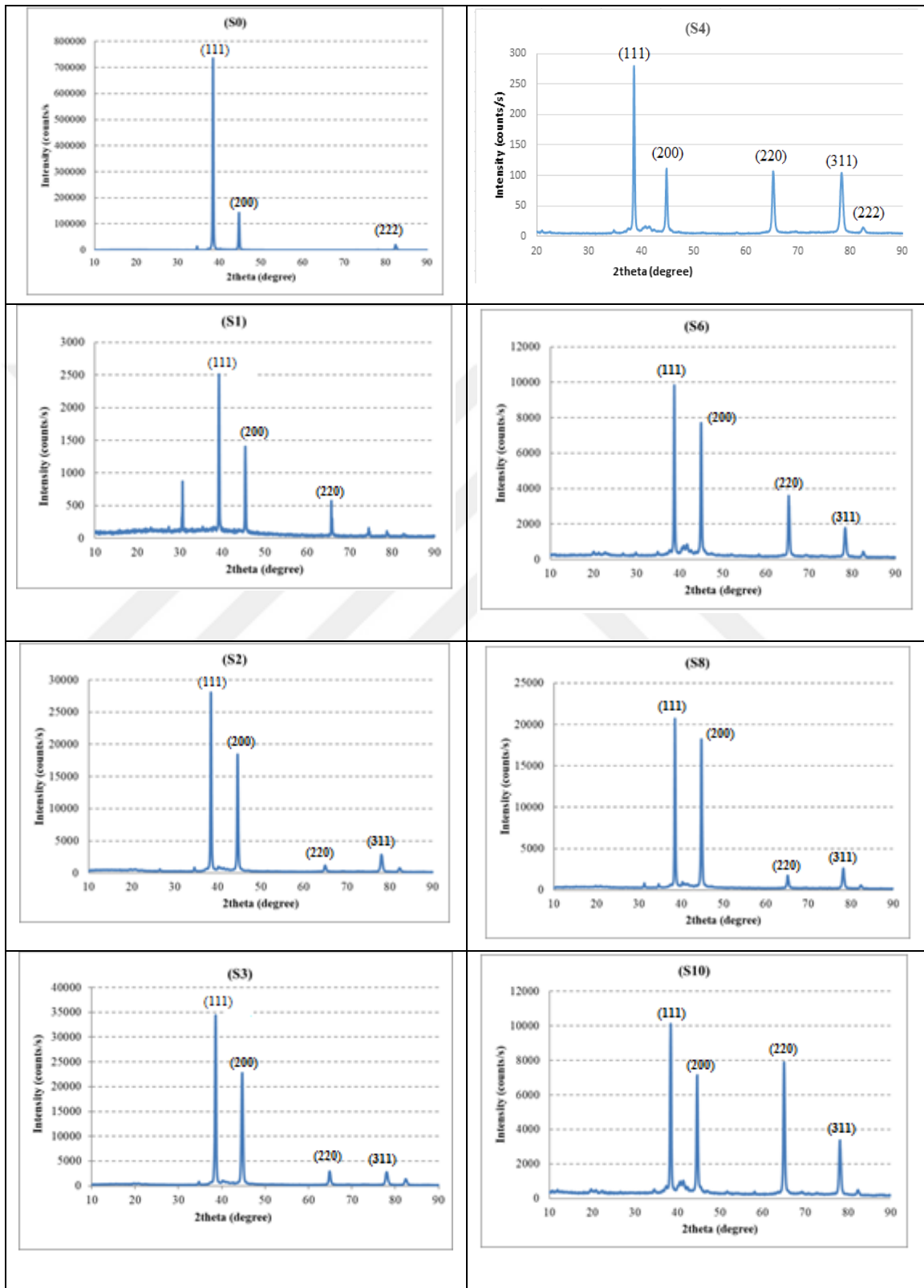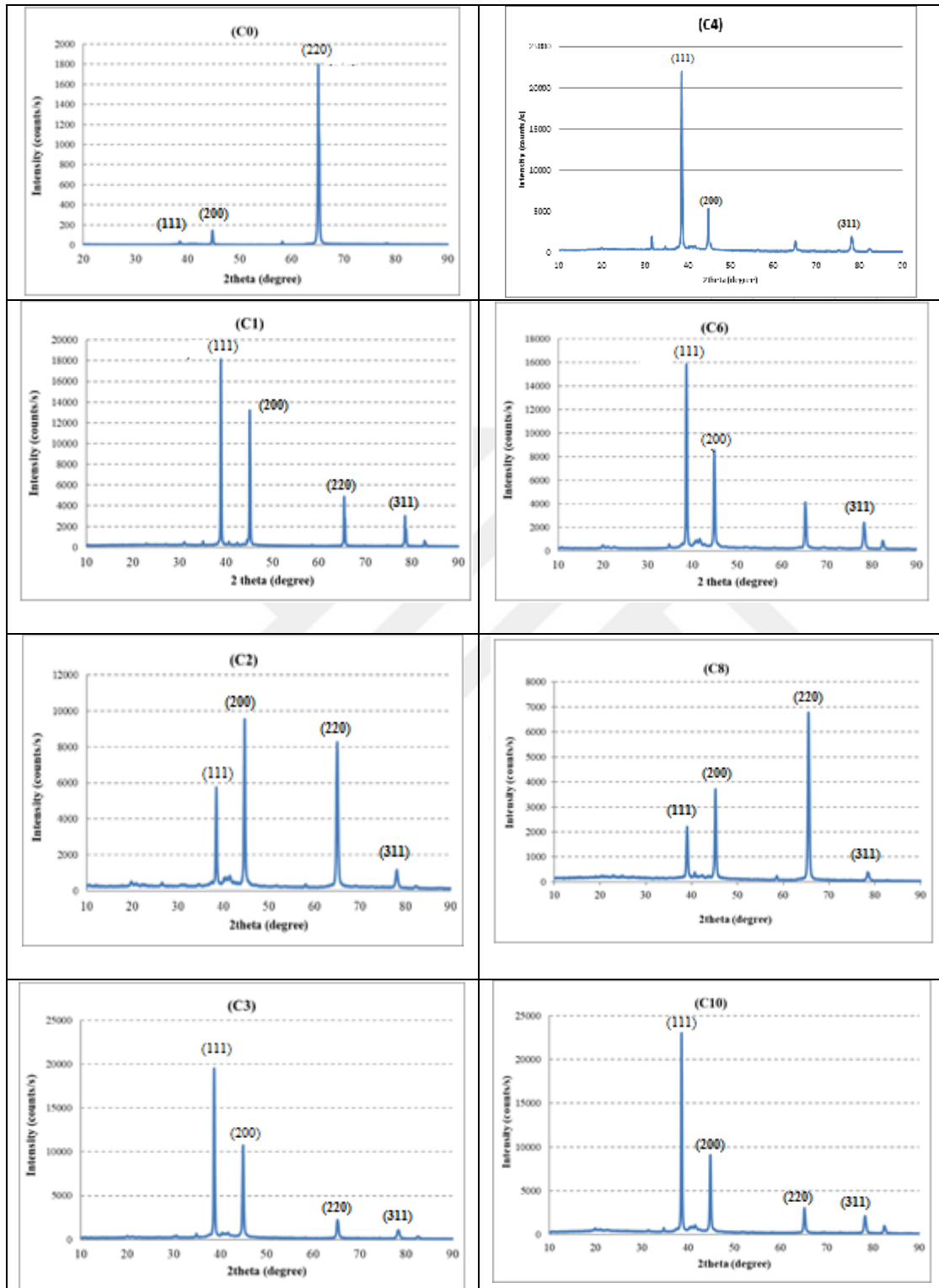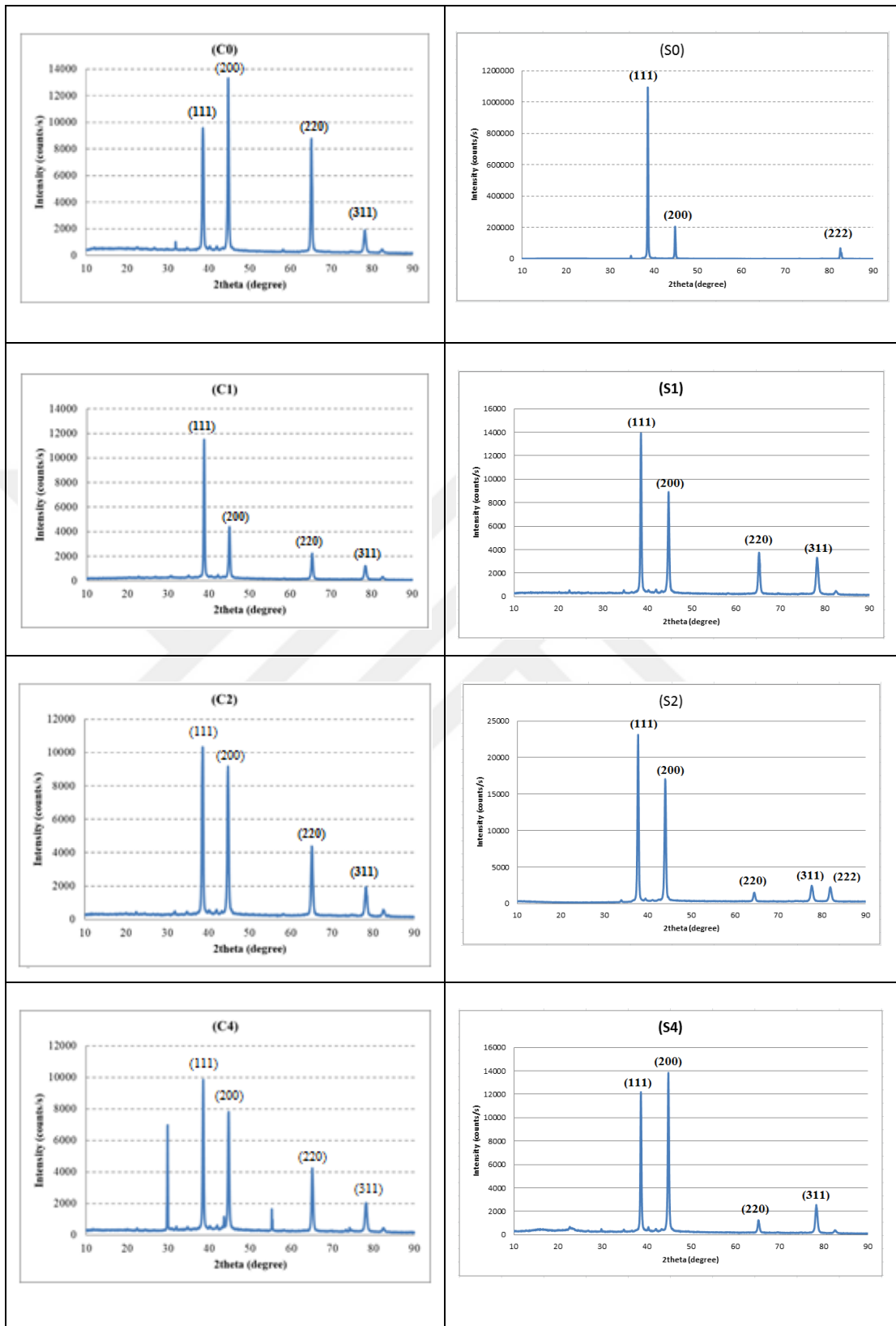
Figure 4.5 : XRD patterns of Al6013 samples in different sections after ECAP.
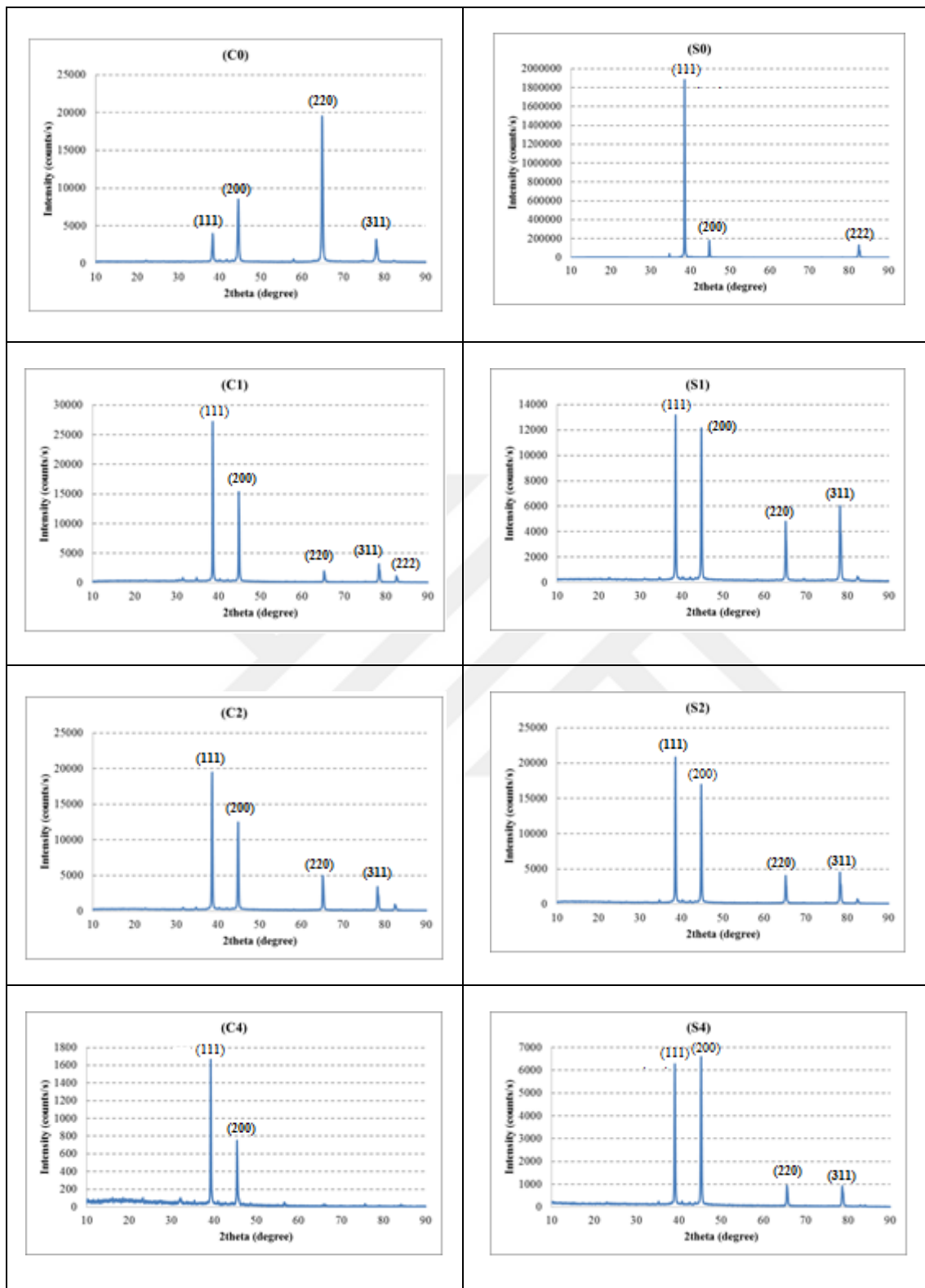
Figure 4.6 : XRD patterns of pure Al samples in different sections after ECAP.

4.2 Microstructural analysis of the samples

In order to do microstructural investigations of the samples by optical and SEM analysis, the Al7075 samples were etched by Keller's solution with chemical etching method as composed of the following proportion: 2 ml HF + 3 ml HCl + 5 ml HNO_3 + 90 ml water.

4.2.1 Optical Microscopy results

Structural changes in the grain and subgrain compositions of ECAPed samples were observed via studies with optical microscope. Grain orientations in rolling direction coming from metal production process were observed on the unpassed sample. In the subsequent passes shearing bands are elongated with the corner stress effect especially can be seen in the longitudinal views. Changes in the grain orientations of ECAPed samples happen while the grain size in the microstructure reduced. Accompanied with the texture evolution and equiaxed grains, passing of the samples can be repeated more than 4 times up to achieving homogeneous and ultrafine grained structure.

By applying image software and conventional measurements, the average size of the grains of Al7075 samples have been reduced from 3μm to about 900 nm at fourth pass in our study (Figure 4.7 - Figure 4.8) .

No pass   4 passes
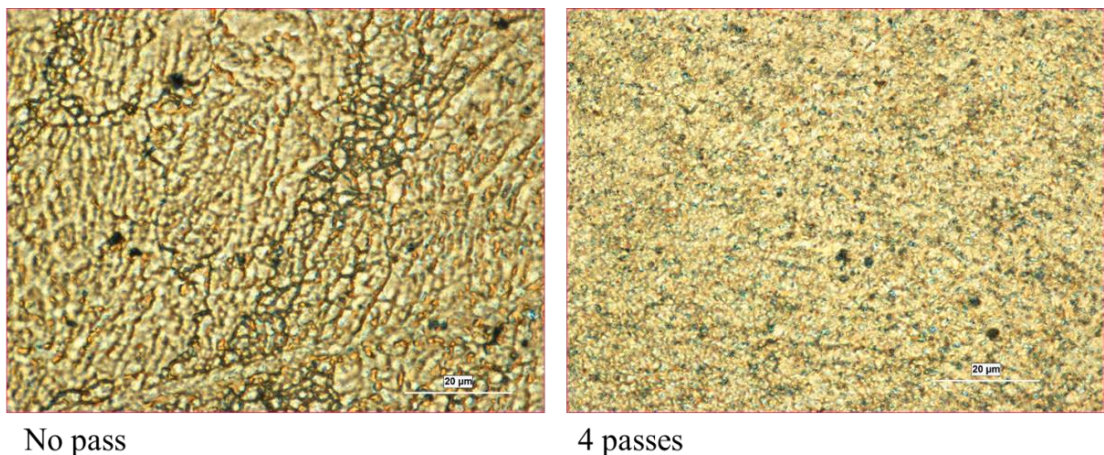
Figure 4.7 : Comparison between microstructures of unpassed and 4th pass cross-sectional surface of Al7075 samples (1000 x).

No pass   4 passes
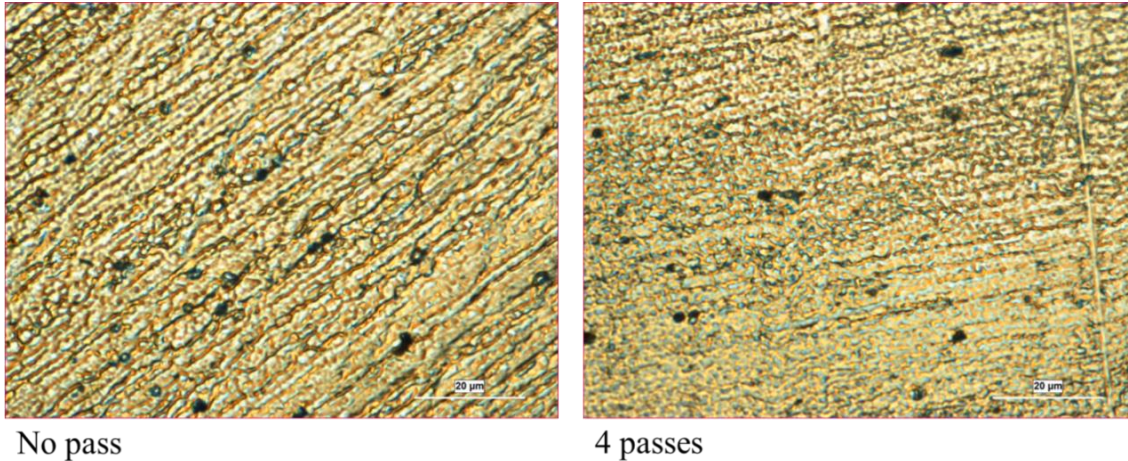
Figure 4.8 : Comparison between microstructures of unpassed and 4th pass longitudinal surface of Al7075 samples (1000 x).

That result doesn't show inconsistency with the previous studies and reports in the literature.

S. M. Kumar et al [24] pressed Al7075 billets through the channel with 90° die angles after annealing at 412 °C for 1 h and then cooled to room temperature. They have observed that the grain diameters reduced from 1.5 μm to 400–440 nm, achieved in route Bc after four passes.

M. Saravanan et al [26] studied on pure aluminum with 90° die angles at room temperature up to eight passes and determined with AFM characterization as the grain sizes reduced from 150 μm to ~620 nm.

It's seen that various parameters such as test material, pass number, die angle and annealing have a potential to make the result different and even better in comparison with our study. Together with the garin division up to achieving uniform distributed ultrafine grains, the impurities and alloy elements have been restricting and as a result the strength of the material has been increasing.

4.2.2 Scanning Electron Microscope (SEM) results

The microstructure of both unpassed and ECAPed samples were studied by SEM microscobe using high-resolution imaging of microstructure analysis. The results of SEM support and are in parallel with optical microscopy data pictures. It's started with shearing bands elongated crystallographically and further equiaxed homogenous

grain formations in the fourth pass. Then the subgrain formation also at the 4th pass and for the sequential passes grain refinement promoted (Figure 4.9) .
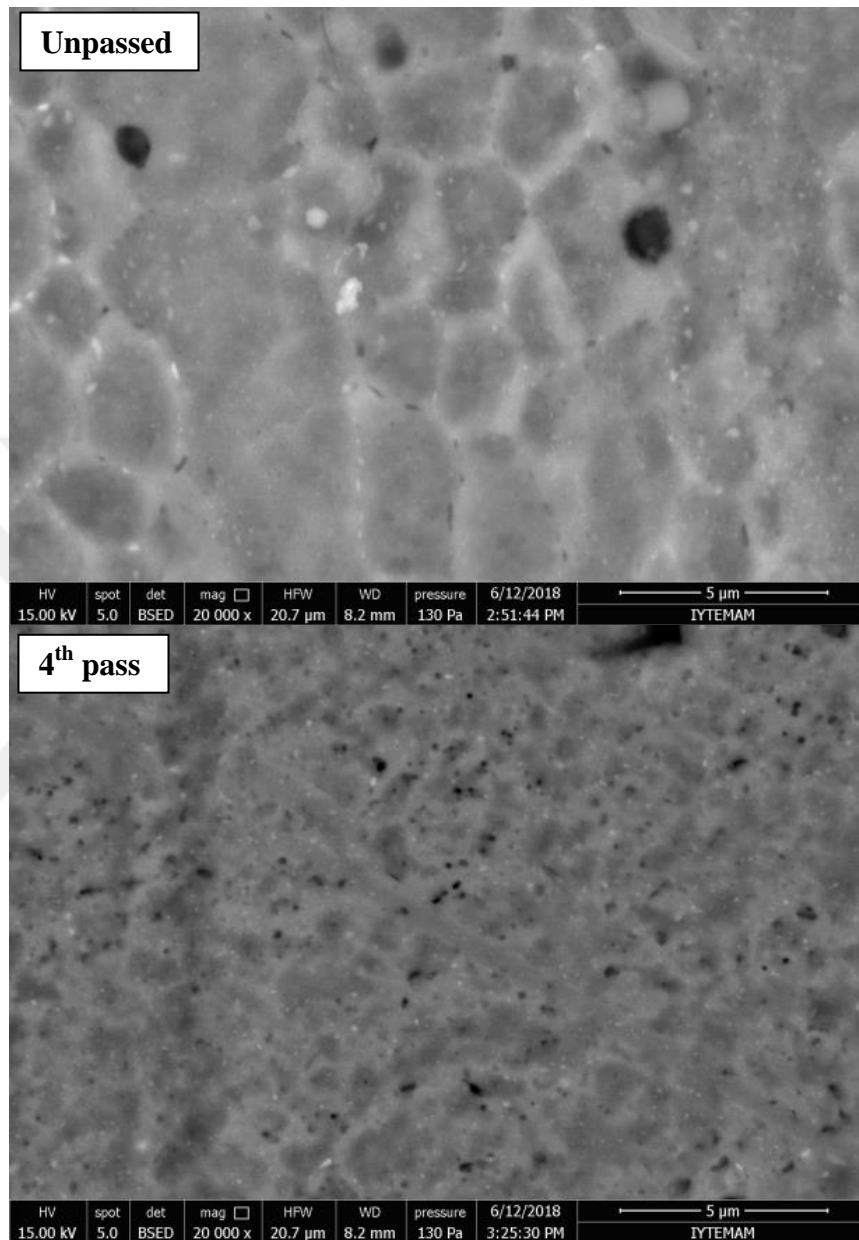
Figure 4.9 : Comparison between microstructures of unpassed and 4th th pass cross-section surface (20,000 x).

The grain dividing and subgrain formation can be seen and followed even though the grain boundaries are not so clear. (Figure 4.10) .
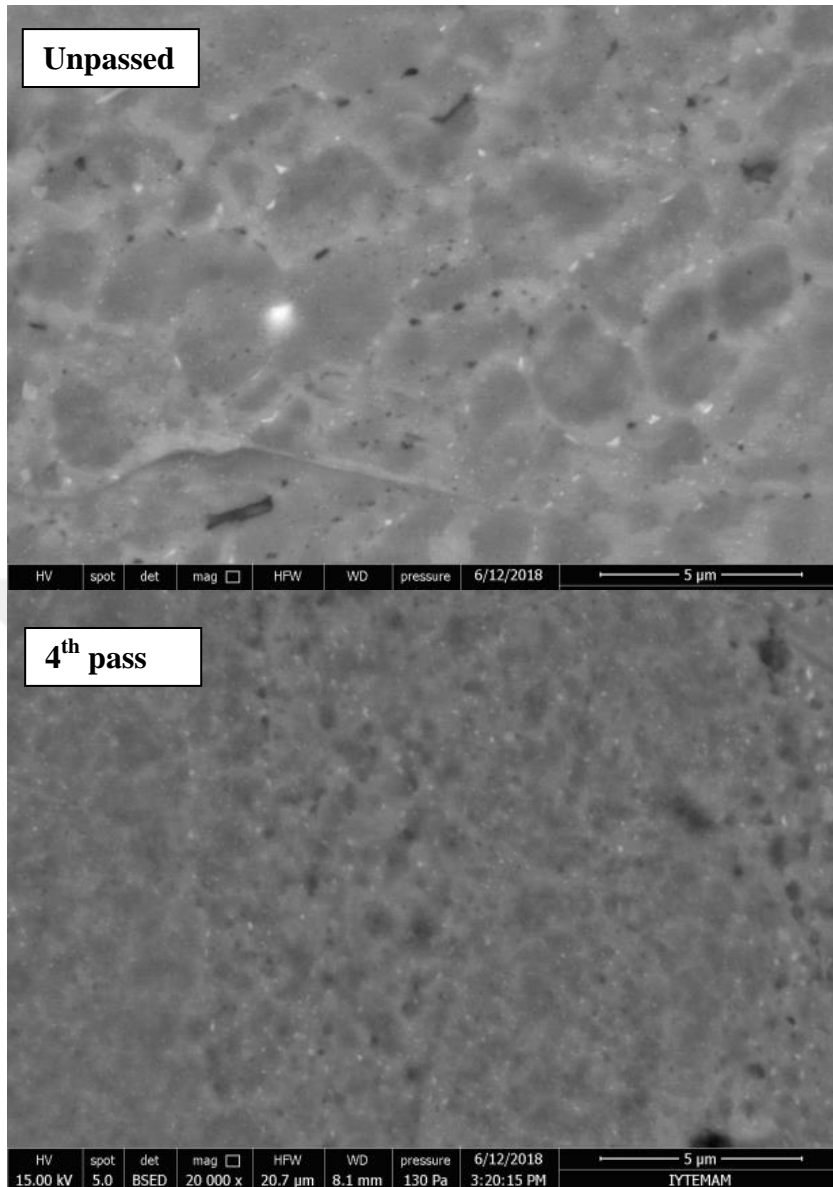
Figure 4.10: Comparison between microstructures of unpassed and 4th pass longitudinal surface (20,000 x).

4.3 Mechanical Properties results

4.3.1 Micro-vickers hardness tests

The mechanical properties of the aluminum alloys have been investigated by applying the micro-vickers hardness test. The hardness values of Al7075, Al6013 and pure Al are given in Figures 4.11 – 4.13, respectively. Also, detailed hardness results of all samples are presented through Table 4.1 to Table 4.3. As can be seen

from Figure 4.11, for Al7075 alloy, the hardness values up to 4th pass after ECAP increases significantly. Even though decreasing in some cases, significant increase in microhardness values were determined for certain gradual passes. With decreasing in dislocation density and the formation of equiaxed grains the low hardness values have been established in certain passing numbers [24].

Hardness values of Al7075 up to 4th pass after ECAP increases significantly from 65HV to 92.4HV as about 30% using Bc route (Figure 4.11) .
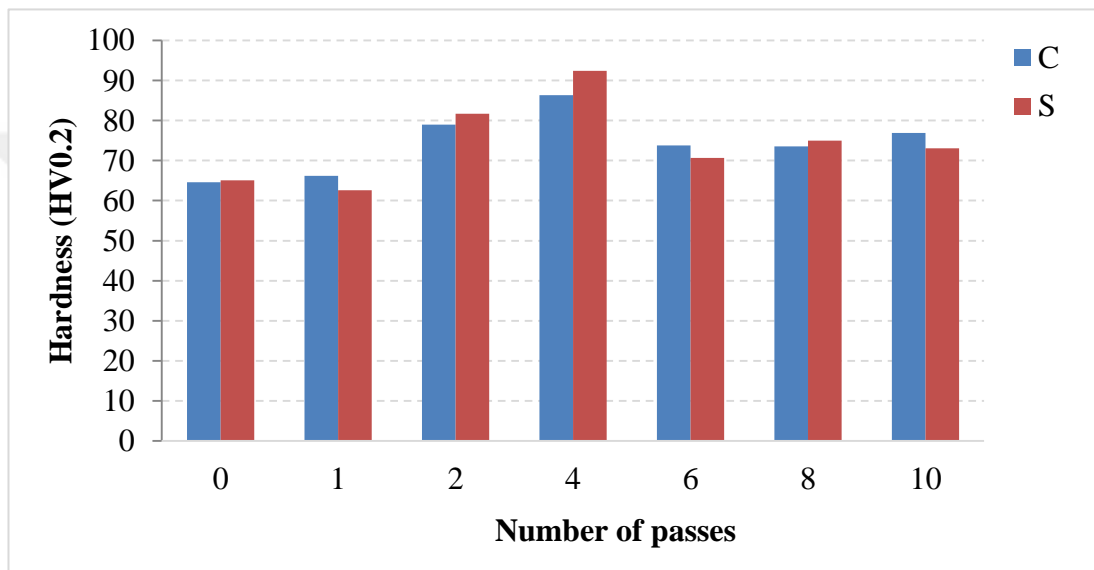
Figure 4.11 : Hardness values versus number of passes of Al7075 samples.

The percentage of increase in quantitative hardness values nearly corresponds to the study done by M. Reddy et al [25] and the study conducted by M. Saravanan et al [26] as mentioned above, however some difference may occur due to variable experimental parameters such as intersection angle, heating temperature, tool design, pressing speed, etc.

A. Güral et al [44] studied on Al7075 alloy with die angle 90° at 200 °C up to 14 passes and observed that hardness values increased up to 4 passes, decreased effectively at 6th pass, again increased 8th pass and then, the hardness was again decreased with dynamic recrystallization. It seem that the results received from this study are also comply with data obtained from our hardness measurements about Al7075 as well.

For pure Al, as can be seen in Figure 4.12, the hardness values up to 4th pass after ECAP increases gradually. Comparing with M. Saravanan et al [26] studies on pure Al mentioned above, as shown in Figure 2.12, the values are increasing gradually just about in the same tendency with our study.
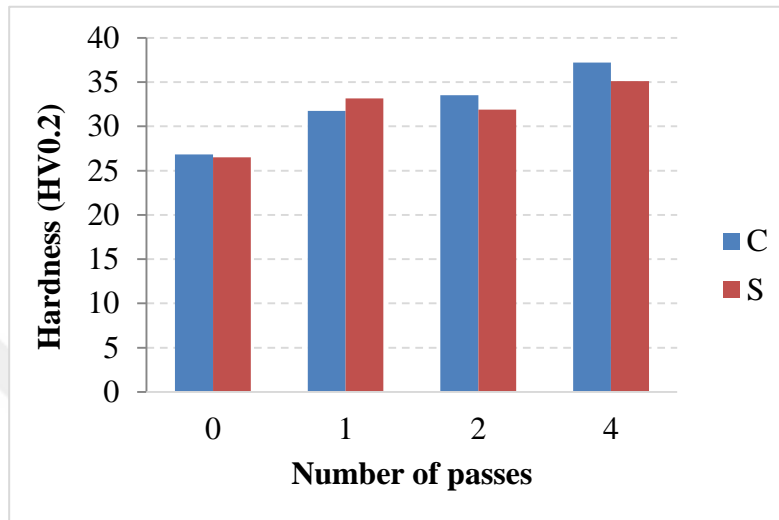
Figure 4.12 : Hardness values versus number of passes of pure Al samples.

As can be seen in Figure 4.13, for Pure Al6013 alloy, the hardness values at the 1st pass increased, then it was observed that the hardness at 2nd and 4th passed samples again decreased nearly to original unpassed values.
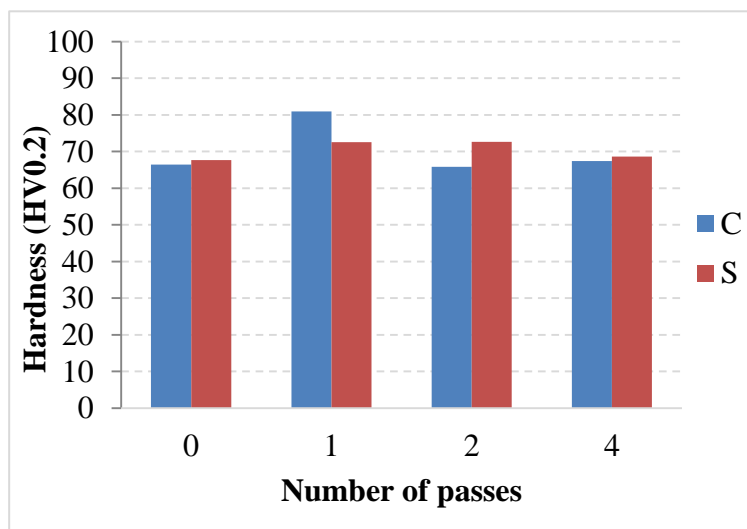
Figure 4.13 : Hardness values versus number of passes of Al6013 samples.

Table 4.1 : Micro-vickers hardness (HV0.2) tests results of Al 7075 alloy.

			Micro Vickers Hardness results (Al 7075)												
	Pass Number:		0		1		2		4		6		8		10	
	Direction:		S	C	S	C	S	C	S	C	S	C	S	C	S	C
Hardness Values (Randomly)		1	63.9	66.9	60.0	63.4	88.0	80.7	78.5	84.1	71.1	80.6	69.2	76.0	70.7	76.5
		2	58.8	62.9	60.9	63.8	83.8	76.0	87.7	85.7	70.1	70.2	71.9	72.4	68.8	72.9
		3	73.1	63.4	61.7	69.9	78.4	73.8	92.9	86.3	72.9	73.9	75.6	74.5	74.4	77.4
		4	63.6	68.0	65.0	66.1	78.9	83.1	98.0	87.4	68.2	71.3	77.0	77.1	74.1	77.4
		5	66.1	61.9	65.3	67.7	79.4	81.5	105.0	88.0	71.1	73.0	81.1	67.8	77.4	80.3
	Average:		65.1	64.6	62.6	66.2	81.7	79.0	92.4	86.3	70.7	73.8	75.0	73.6	73.1	76.9
	Std.deviation:		5.2	2.7	2.4	2.7	4.1	3.9	10.1	1.5	1.7	4.1	4.6	3.7	3.4	2.7

Table 4.2 : Micro-vickers hardness (HV0.2) tests results of Pure Al.

			Micro Vickers Hardness results (Pure Al)							
	Pass Number:		0		1		2		4	
	Direction:		S	C	S	C	S	C	S	C
Hardness Values (Randomly)		1	26.0	27.6	32.1	34.4	29.3	30.2	35.7	37.6
		2	22.8	27.1	35.5	29.0	31.1	38.5	34.7	37.9
		3	29.0	25.9	35.7	32.2	36.6	35.5	34.4	33.6
		4	29.4	26.9	28.7	33.4	31.6	31.5	33.2	39.0
		5	25.3	26.6	33.9	29.7	30.9	31.9	37.6	38.0
	Average :		26.5	26.8	33.2	31.7	31.9	33.5	35.1	37.2
	Std.deviation :		2.7	0.6	2.9	2.3	2.8	3.4	1.6	2.1

Table 4.3 : Micro-vickers hardness (HV0.2) tests results of Al6013 alloy.

			Micro Vickers Hardness results (Al 6013)							
	Pass Number:		0		1		2		4	
	Direction:		S	C	S	C	S	C	S	C
Hardness Values (Randomly)		1	69.4	70.6	73.8	87.0	69.0	68.6	54.7	74.1
		2	67.7	62.9	68.8	81.0	68.0	61.2	71.0	66.8
		3	63.1	67.1	74.4	79.0	81.8	65.9	68.7	69.8
		4	72.3	66.5	69.7	83.0	71.3	63.4	81.9	60.8
		5	65.9	64.9	76.0	74.8	73.2	70.2	66.8	65.5
	Average :		67.7	66.4	72.5	81.0	72.7	65.9	68.6	67.4
	Std.deviation :		3.5	2.9	3.1	4.5	5.5	3.7	9.7	5.0

4.3.2 Nanoindentation tests

As a result of the nanoindentation tests for unpassed sample and 4th passed sample, different hardness and elasticity modulus values of different loads were determined

41

and the mechanical property changes were observed in the sample before and after the process.

It is observed that the mechanical properties at 4th pass of ECAP process for Al7075 are started to change. Grains started to be divided towards subgrains and the material has a tendency to be more strengthened. The subgrain formation and grain refinement is started but evolution of homogenious structure has not been achieved yet. Due to variable experimental parameters some deviations are prevailing and the results came from nanoindentation tests are not get completely along with Micro-vickers hardness test results (Figure 4.14 - Figure 4.17) .
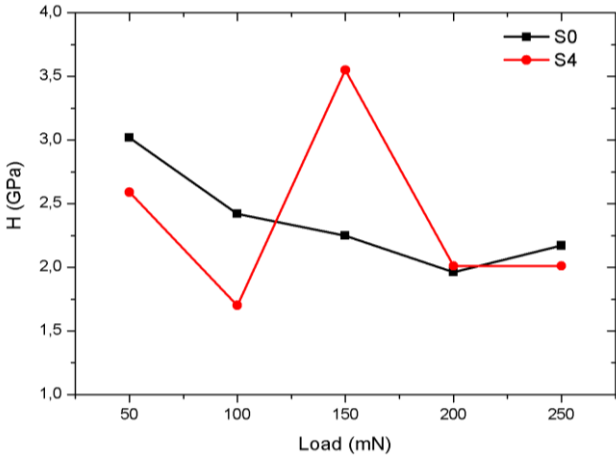
Figure 4.14 : Load – Hardness graph for cross-section of no pass and four passed Al7075 samples.
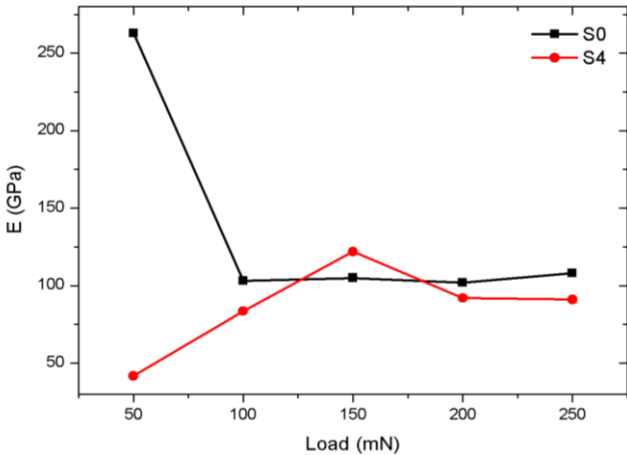
Figure 4.15 : Load – Elasticity modulus graph for cross-sections of no pass and four passed Al7075 samples.
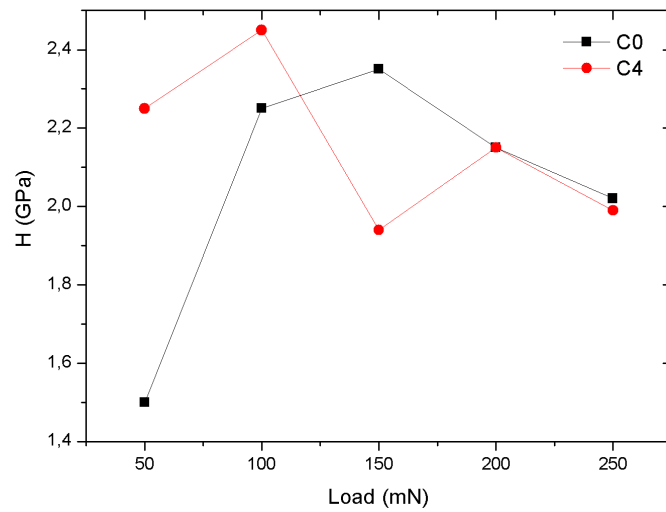
Figure 4.16 : Load – Hardness graph for longitudinal sections of no pass and four passed Al7075 samples.

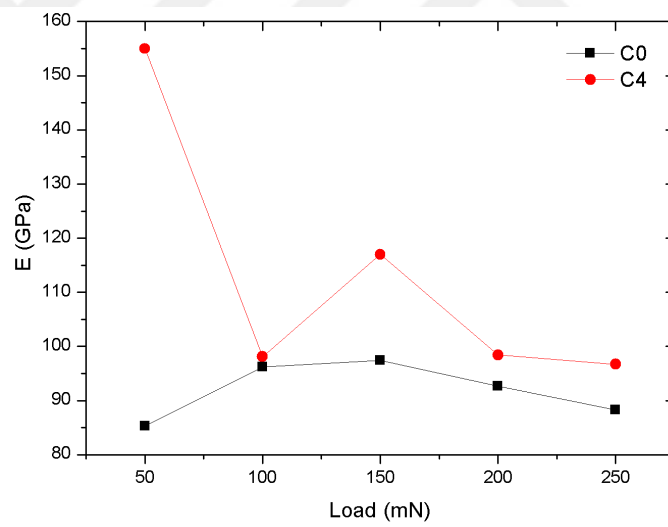**Figure 4.17 :** Load – Elasticity Modulus graph for longitudinal sections of no pass and four passed Al7075 samples.

5. CONCLUSION

All the main parameters, especially the die design and convenient lubrication should be considered meticulously. Besides to assure optimum mechanism, it was realized that any deviation from any parameter in the progress may have unfavorable and serious effects on the results. Every detail must be taken into consideration pre or after each step.

At the beginning of the trials we intended to make a wide comprehensive experimental ECAP investigation on certain Al alloys as Al 7075, Al 6013 and pure Al. Due to its importance and extensive industrial application field we decided to progress in detail with Al 7075 alloy as the main experimental material and the others two are as supportive. Al 7075 alloy samples have been ECAPed up to 10 passes and the others up to 4 passes. XRD diffraction patterns obtained from all the analyzes exhibit individual spectacular changes in peak configurations and crystallographic orientations for each pressed sample. Scherrer formula calculations shown that the remarkable decrease in the crystal size. Optical microscopy and SEM images also support XRD analyzes results with respect to the grain size refinement. Micro-vickers hardness tests results and Nanoindentation tests results have shown that the mechanical properties of the ECAPed samples usually improved.

It is a fact that the data could be more satisfactory and the results could be better. Owing to it was the first experience done with that new ECAP tools, we faced many failures and spent rather times up to achieve some successful intended goals. The constructual experiences obtained in this study may provide several contributions to starter researchers.

It has been encountered that Al and its alloys are prone to oxidation. To cope this handicap, all the microscopic appointment and relating devices need to get ready just after polishing the samples. Microscopic inspections should be started immediately after polishing and should be completed as soon as possible.

Graphite based oil has been used for lubrication prior to each cyclic procedure, but it has been perceived that the use of derivatives such as molybdenum disulfide (MoS_2)

could give better achievements. Due to its vital importance, just before starting the experiment the decision about the lubrication type must had been taken consciously.

Additionally, ECAP process can be combined with any other SPD techniques to achieve better mechanical and functional properties. The material can be cured by aging or any thermomechanical processing before or after the experiment.

It's necessary to continue in progressing the pass number up to achieving a homogeneous, equiaxed and ultrafine grained structure. For various channel angles ideal pass number may be different. For example while 90 degree channel angle would require 8 passes for the finest structure, 120 degree channel angle may need more passes for a totally equiaxed grain and homogenous structure.

Strength and ductility are the essential mechanical characteristics for the metallic materials. They are seem as reciprocal each other. Metallics have been handling and evaluating as they strong or ductile, but infrequently both at once. Plenty of ECAP experiments have shown that reducing the structure of the material to nano levels results in an exceptional combination of high strength and ductility all at once [42]. ECAP technique has been now achieved an important stage in processing of UFG metallic materials. A huge literature from all over the world and plenty of laboratory experimental results have a high innovation potential available to apply manufacturing lines and emerge patented inventions. Accordingly, significant new innovative developments have been expecting in the manufacturing superplastic UFG nanoengineering products [43].

Even though it is a novel technique many scientific investigation had been conducted and characterized using various kinds of ECAP process. There are existing plenty of scientific and experimental investigations waiting for transferring to industrial production. All of the literature need to be reviewed to prepare overall standardisations for applicable elements. So the industrialisation and commercialization of ECAP will achieve to a point which it deserved. ECAP process has the potential to trigger many developments in manufacturing industries such as mechanical, electrical and chemical fields in the next periods.

REFERENCES

[1] Valiev, R.Z., & Langdon, T.G. (2006). Principles of equal-channel angular pressing as a processing tool for grain refinement. *Prog. Mater. Sci., 51(7):881-981.*

[2] http://asm.matweb.com/search/SpecificMaterial.asp?bassnum=MA7075T6 (accessed 19 July 2018).

[3] http://www.aluminumalloyplate.com (accessed 19 July 2018).

[4] Segal, V. M. (1977). The method of material preparation for subsequent Working. USSR Patent 575892.

[5] Dowling, N. E. (2013). Mechanical Behavior of Materials – Engineering Methods for Deformation, Fracture, and Fatigue, fourth edition. *Pearson Education Limited.*

[6] Callister, Jr, W. D. (2004). Materials Science and Engineering – An introduction, seventh edition. *John Wiley & Sons, Inc.*

[7] Valiev, R., Z., Islamgaliev, R.,K., & Alexandrov, I., V. (2000). Bulk nanostructured materials from severe plastic deformation. *Progress in Materials Science 45, 103-189.*

[8] Estrin, Y., & Vinogradov, A. (2013). Extreme grain refinement by severe plastic deformation: A wealth of challenging science. *Acta Materialia 61, 782–817.*

[9] Nakashima, K., Horita, Z., Nemoto, M., & Langdon, T.G. (2000). Development of a Multi-Pass Facility for Equal-Channel Angular Pressing to High Total Strains. *Materials Science and Engineering A, 281, 82-87.*

[10] Purcek, G., Yanar, H., Shangina, D.,V., Demirtas, M., Bochvar, N.,R., & Dobatkin, S.,V. (2018). Influence of high pressure torsion-induced grain refinement and subsequent aging on tribological properties of Cu-Cr-Zr alloy. *Journal of Alloys and Compounds 742, 325-333. doi: https://doi.org/10.1016/j.jallcom.2018.01.303*

[11] Han, S., Lim, C., Kim, C., & Kim, S., (2005). The microstructural evolution during the equal channel angular pressing process and its relationship with the tensile behavior of oxygen-free copper. *Metallurgical and Materials Transactions A, Volume 36, Issue 2, pp 467–4. doi:*

https://doi.org/10.1007/s11661-005-0318-6

[12] Ferrasse, K., S., Hartwig, K., T., Goforth, R., E., & Segal, V., (1997). Microstructure and properties of copper and aluminum alloy 3003 heavily worked by equal channel angular extrusion. *Metallurgical and Materials Transactions A 28(4):1047-1057. doi:* 10.1007/s11661-997-0234-z

[13] Cordero, Z., C., Knight, B., E., & Schuh, C., A., (2018). Six decades of the Hall–Petch effect – a survey of grain size strengthening studies on pure metals. *Department of Materials Science and Engineering, MIT, Cambridge MA 02139. doi:* https://doi.org/10.1080/09506608.2016.1191808

[14] Pande, C., S., & Cooper, K.P. (2009). Nanomechanics of Hall–Petch relationship in nanocrystalline materials. *Progress in Materials Science, 54, 689–706.*

[15] Carlton, C., E., & Ferreira, P., J. (2007). What is behind the inverse Hall–Petch effect in nanocrystalline materials? Acta Materialia, 55, 3749–3756.

[16] Padmanabhan, K., A., Sripathi, S., Hahn, H., & Gleiter, H. (2014). Inverse Hall–Petch effect in quasi-and nanocrystalline materials. *Materials Letters, 133, 151–154.*

[17] Starink, M., J. (2017). Dislocation versus grain boundary strengthening in SPD processed metals: Non causal relation between grain size and strength of deformed polycrystals. *Materials Science & Engineering A 705, 42–45.*

[18] Mohammadabadi, A., S., & Dehghani, K. (2008). A New Model for Inverse Hall-Petch Relation of Nanocrystalline Materials. *Journal of Materials Engineering and Performance 662—Volume 17. doi:* 10.1007/s11665-008-9206-8

[19] Hall, E.O. (1951). The deformation and ageing of mild steel: III discussion of results. *Proc. Phys. Soc. B 64 747–753.*

[20] Hansen, N., (2004). Hall–Petch relation and boundary strengthening. *Scripta Materialia, 51, 801–806.*

[21] Quek, S., S., Chooi, Z., H., Wu, Z., Zhang, Y., W., & Srolovitzc, D., J. (2016). The inverse hall–petch relation in nanocrystalline metals: A discrete dislocation dynamics analysis. *Journal of the Mechanics and Physics of Solids Volume 88, Pages 252-266.*

[22] Comaneci, R., Chelariu, R., & Zaharia, L., (2008). Processing of Aluminium and Al-Mg Alloys by Severe Plastic Deformation. *Metal 2008 13.*

[23] Furukawa, M., Horita, Z., Nemoto, M., Ravisankar, B., & Langdon, T., G. (2001) Processing of metals by equal-channel angular pressing. *Journal of materials science 36, 2835 – 2843*

[24] Kumar, S., M., Gudimetla, K., Venketachalam, P., Ravisankar, B., & Jayasankar, K. (2012) Microstructural and mechanical properties of Al 7075 alloy processed by equal channel angular pressing. *Mater. Sci. Eng., A, 533, 50 54.*

[25] Reddy, M., Kumar, M., S., & Kumar, V., A. (2013). Improving Mechanical Properties of AL 7075 alloy by Equal Channel Angular Extrusion process. *International Journal of Modern Engineering Research (IJMER), Vol. 3, Issue. pp-2713-2716.*

[26] Saravanan, M., Pillai, V., B., Pai, V., Brahmakumar, M., & Ravi., K., R., (2016). Equal channel angular pressing of pure aluminium-an analysis. *Bull. Mater. Sci., Vol. 29, No. 7, pp. 679–684. © Indian Academy of Sciences.*

[27] https://www.azom.com/article.aspx?ArticleID=8611 (accessed 19 July 2018).

[28] ftp://161.24.15.247/Montestruque/EST-25/LAB-4/AR-MMPDS-01_CAP8.pdf (accessed 19 July 2018).

[29] http://www.seykoc.com.tr/icerik/alloys-1050-seykoc-aluminium?dil=en (accessed 19 July 2018).

[30] Kamachia, M., Furukawa, M., Zenji, H., & Langdon, T., G., (2003). Equal-channel angular pressing using plate samples. *Materials Science and Engineering A361 (2003) 258–266.*

[31] Güral, A., Tekeli, S., Aytaç, A., & Karataş, Ç., (2011). Construction of an Equal Channel Angular Pressing Unit and Determination of Optimum Parameters for Al-Zn-Mg-Cu Alloy Chosen as A Modal Material. *Journal of Polytechnic, Vol: 14 No: 4 pp. 243-248.*

[32] Yamashita, A., Yamaguchi, D., Horita, Z., & Langdon, T., G., (2000). Influence of pressing temperature on microstructural development in equal-channel angular pressing. *Materials Science and Engineering A287, 100–106.*

[33] Segal, V. M. (2003). Slip line solutions, deformation mode and loading history during equal channel angular extrusion. *Materials Science and Engineering A345, 36-46.*

[34] Frint, P. M. F., Wagner, X., Weber, S., Seipp, S., Frint, S., & Lampke, T., (2016). An experimental study on optimum lubrication for large-scale severe plastic deformation of aluminum-based alloys. *Journal of Materials Processing Technology 239 (2017) 222–22.*

[35] http://www.petrofer.com.tr (accessed 19 July 2018).

[36] Agwa, M., A., Ali, M., & Amal, E., (2016). Optimum processing parameters for equal channel angular pressing. *Mechanics of Materials 100, 1–11.*

[37] Venkatachalam, P., Kumar, S., R., Ravisankar, B., Paul, V., T., & Vijayalakshmi, M., (2010). Effect of processing routes on microstructure and mechanical properties of 2014 Al alloy processed by equal channel angular pressing. *Trans. Nonferrous Met. Soc. China 20(2010) 1822−1828.*

[38] Furukawa, M., Iwahashi, Y., Horita, Z., Nemoto, M., & Langdon, T., G., (1998). The shearing characteristics associated with equal channel angular pressing. *Materials Science and Engineering A257, 328–332.*

[39] Langdon, T., G., (2013). Twenty-five years of ultrafine-grained materials: Achieving exceptional properties through grain refinement. *Acta Materialia 61, 7035–7059.*

[40] Segal, V. M. (1999). Equal channel angular extrusion: from macromechanics to structure formation. *Materials Science and Engineering A271, 322–333.*

[41] Cullity, B., D. (1978). Elements of X-Ray Diffraction. *Addison-Wesley Publishing Company, Inc.*

[42] Valiev, R., (2004). Nanostructuring of metals by severe plastic deformation for advanced properties. *Nature materials, Vol 3.*

[43] Huang, Y., & Langdon, T., G., (2013). Advances in ultrafine-grained materials. *Materials Today, Volume 16, Number 3.*

[44] Güral, A., Tekeli, S., Aytaç, A., & Türkan, M., (2012). Microstructural Characterization Of 7075 Aluminum Alloy Severe Deformed By Equal Channel-Angular Pressing (ECAP). *Journal of the Faculty of Engineering and Architecture of Gazi University, Vol 27, No 4, 807-812.*
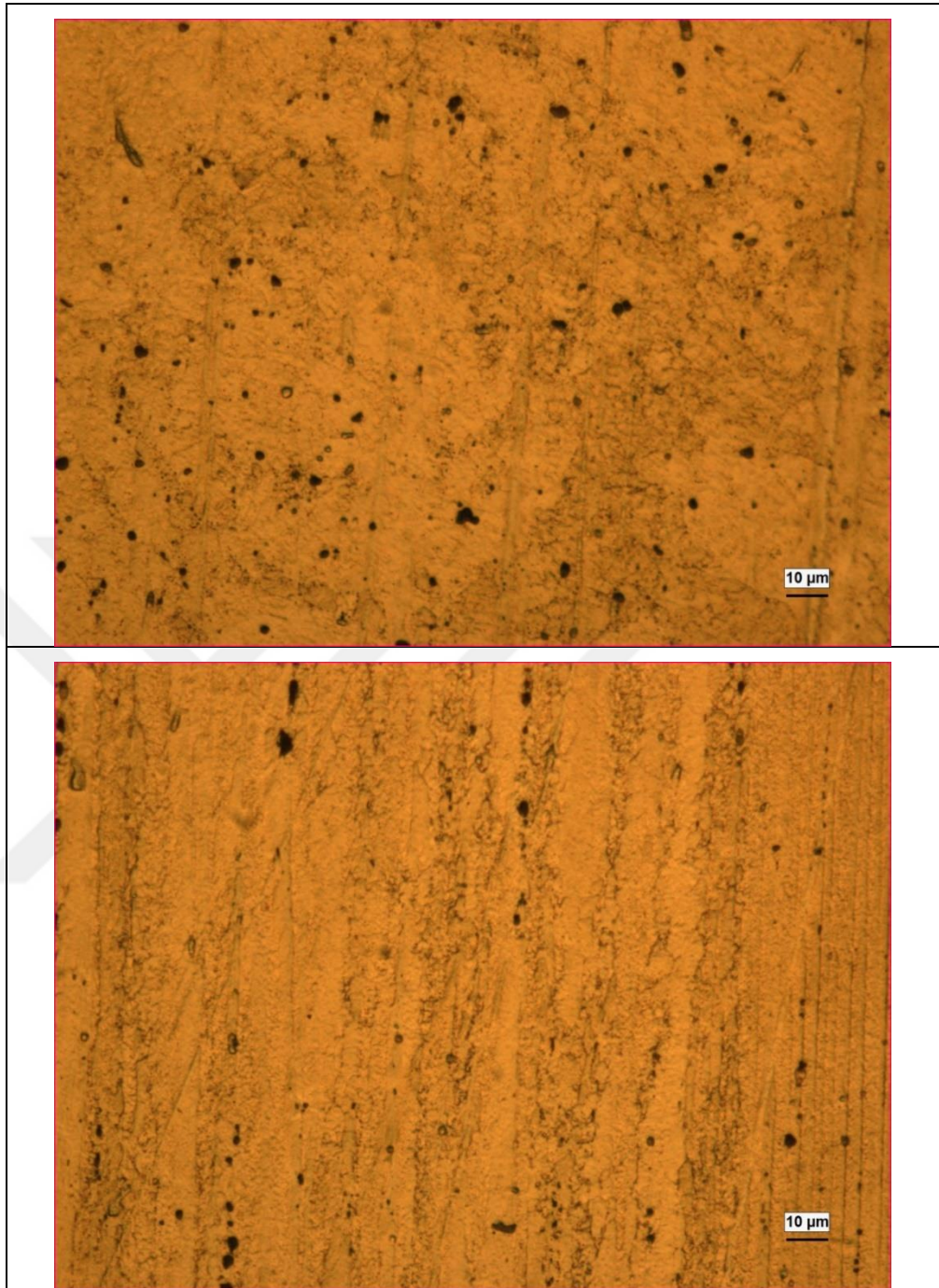
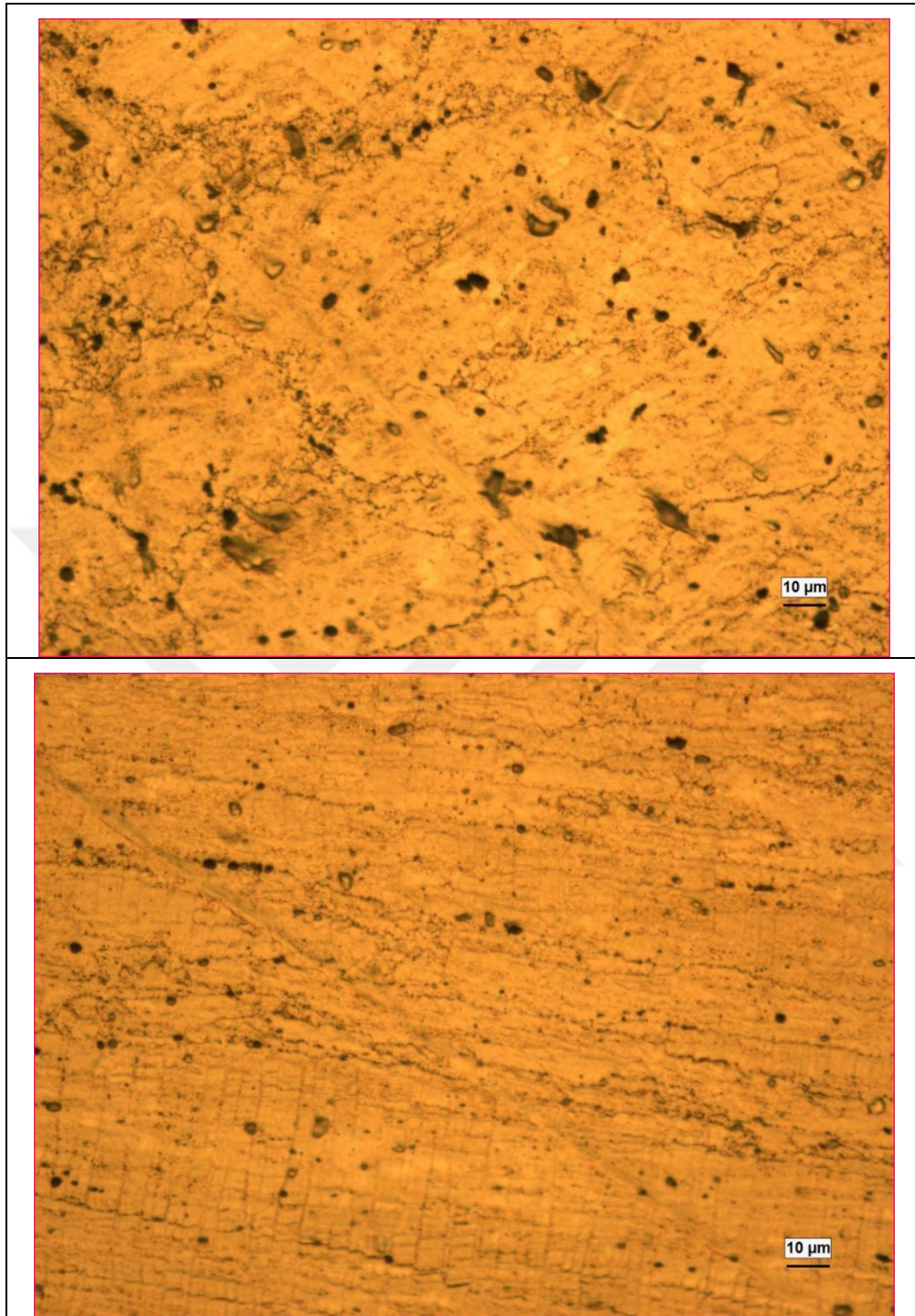**Appendix-01**

OPTICAL MICROSCOPY RESULTS
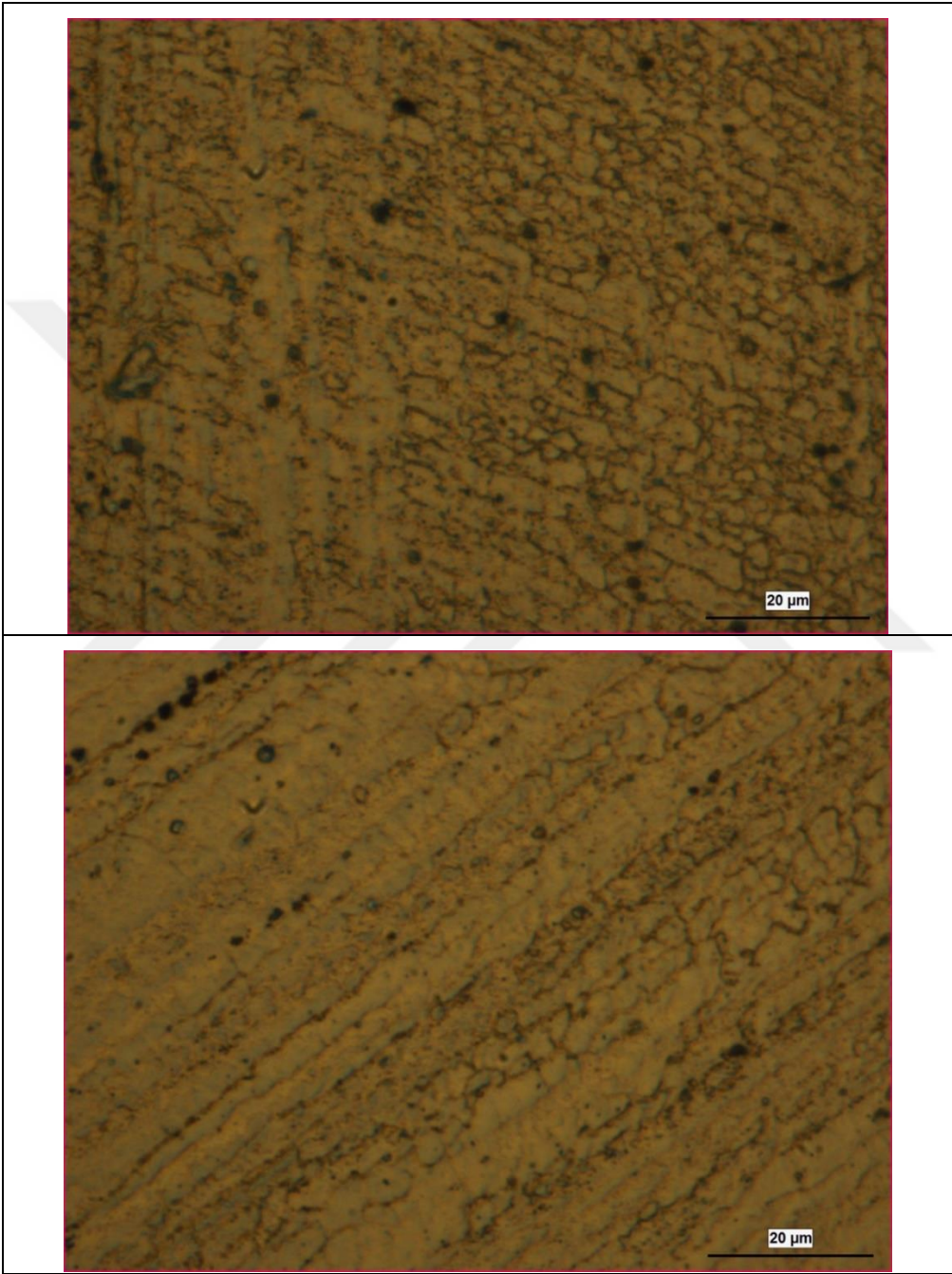
Figure A1.1 : Optical microscope images taken at 1000X from different cross-sections (a. S and b. C surfaces) of 2 passed Al7075 samples.

Figure A1.2 : Optical microscope images taken at 500X from different cross-sections (a. S and b. C surfaces) of 8 passed Al7075 samples.
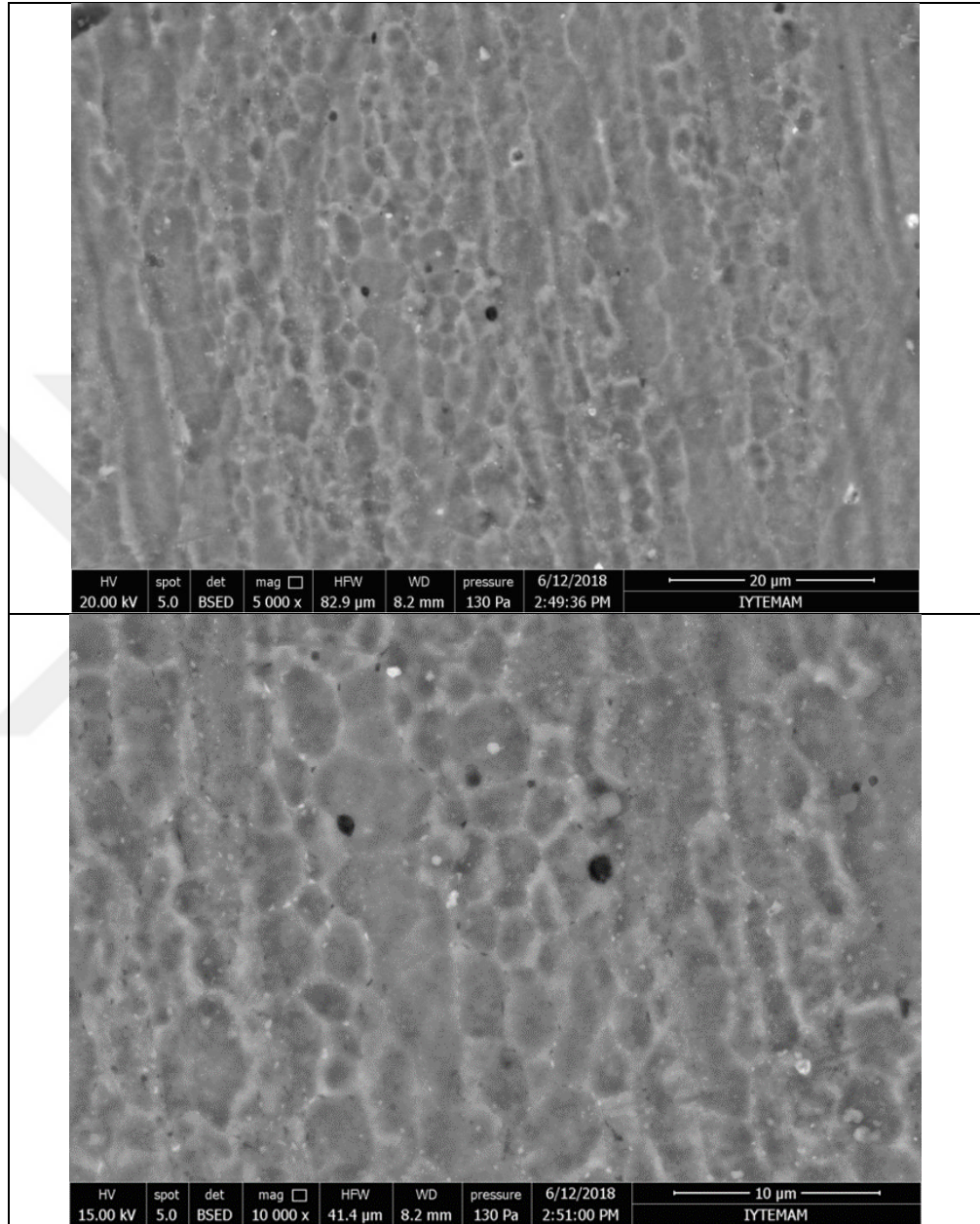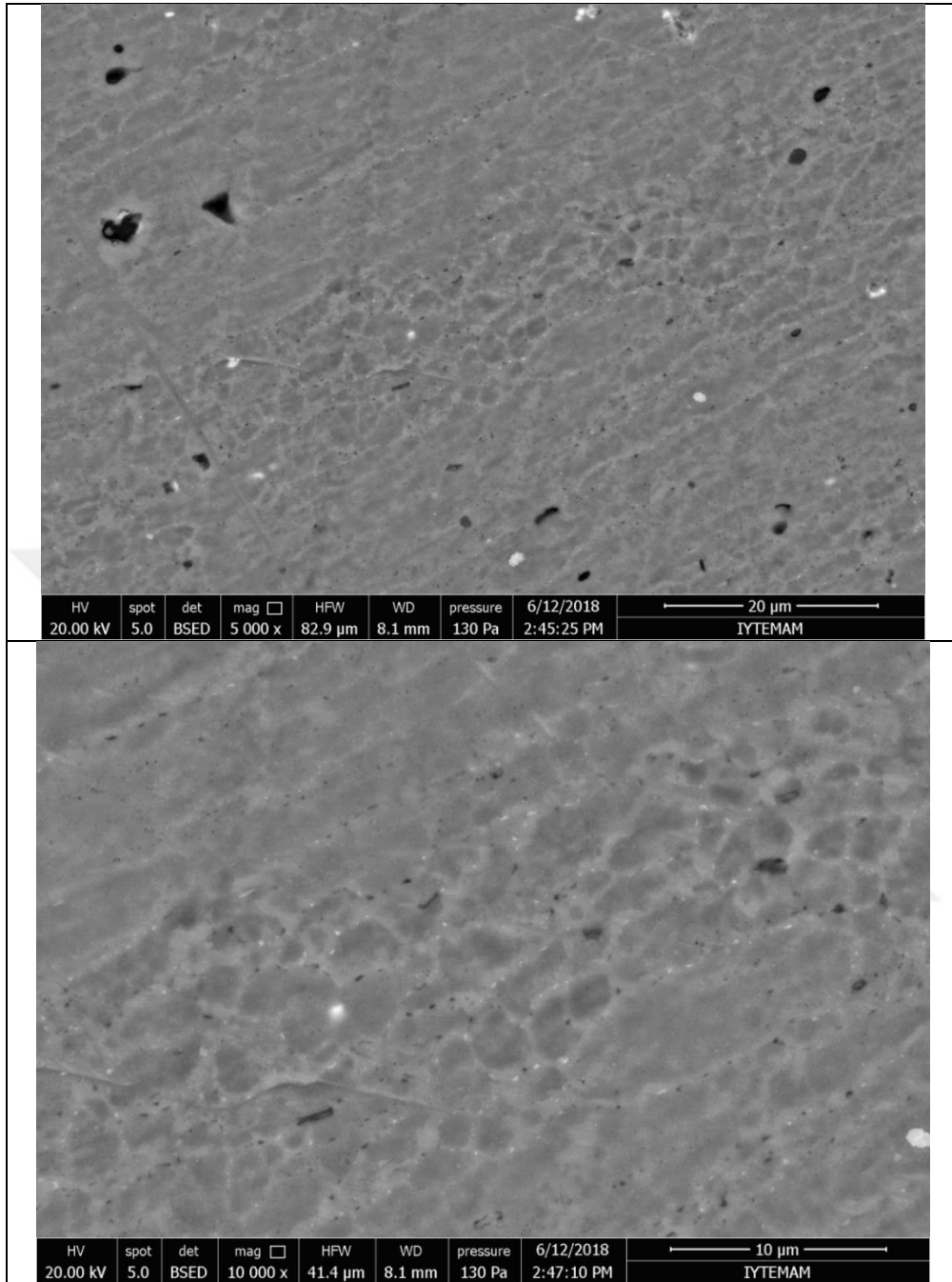
Figure A1.3 : Optical microscope images taken at 500X from different cross-sections (a. S and b. C surfaces) of 10 passed Al7075 samples.
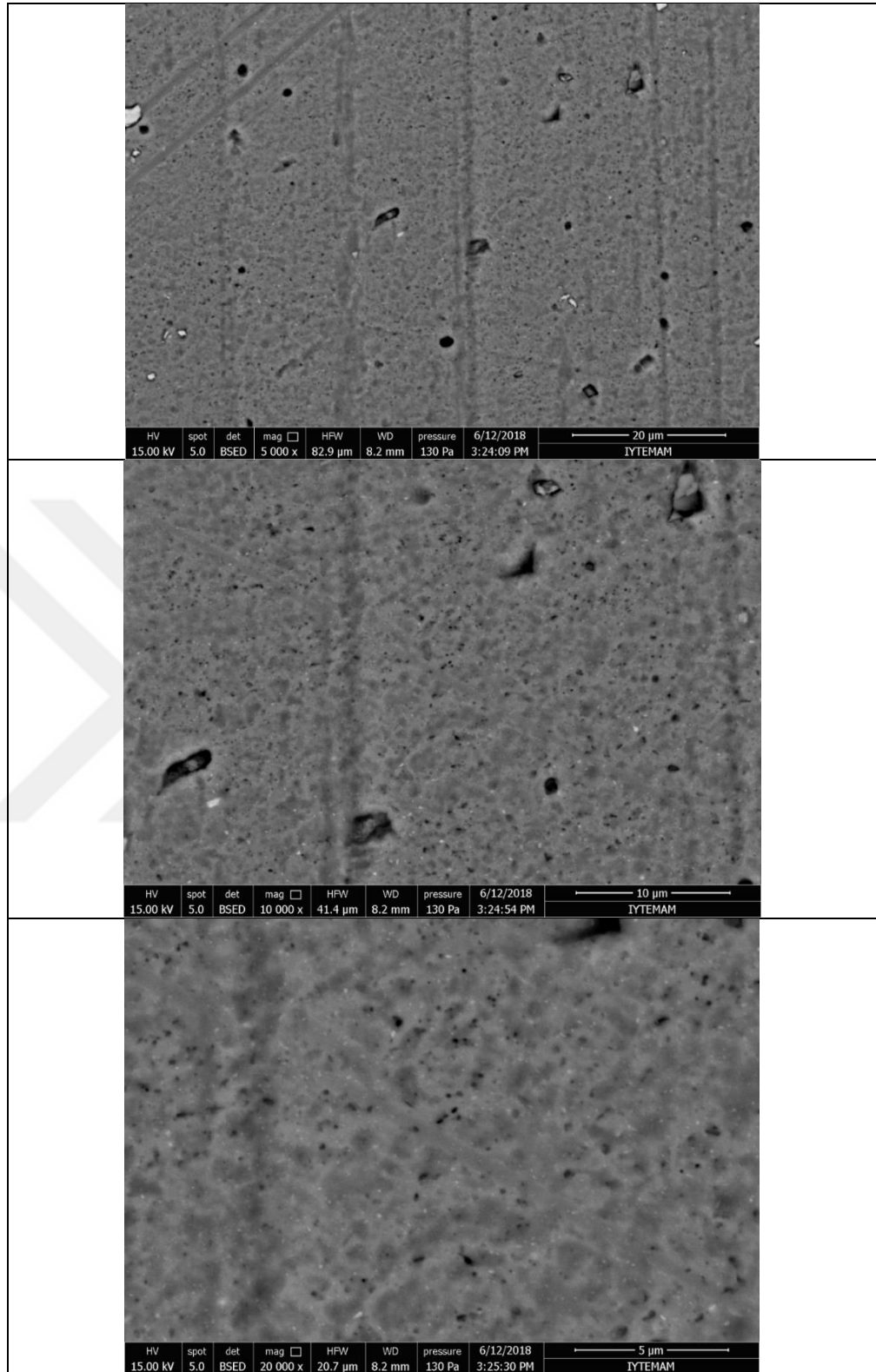
52

SEM RESULTS

Figure A2.1 : SEM images taken from S surface at different magnifications of no pass Al7075 samples.
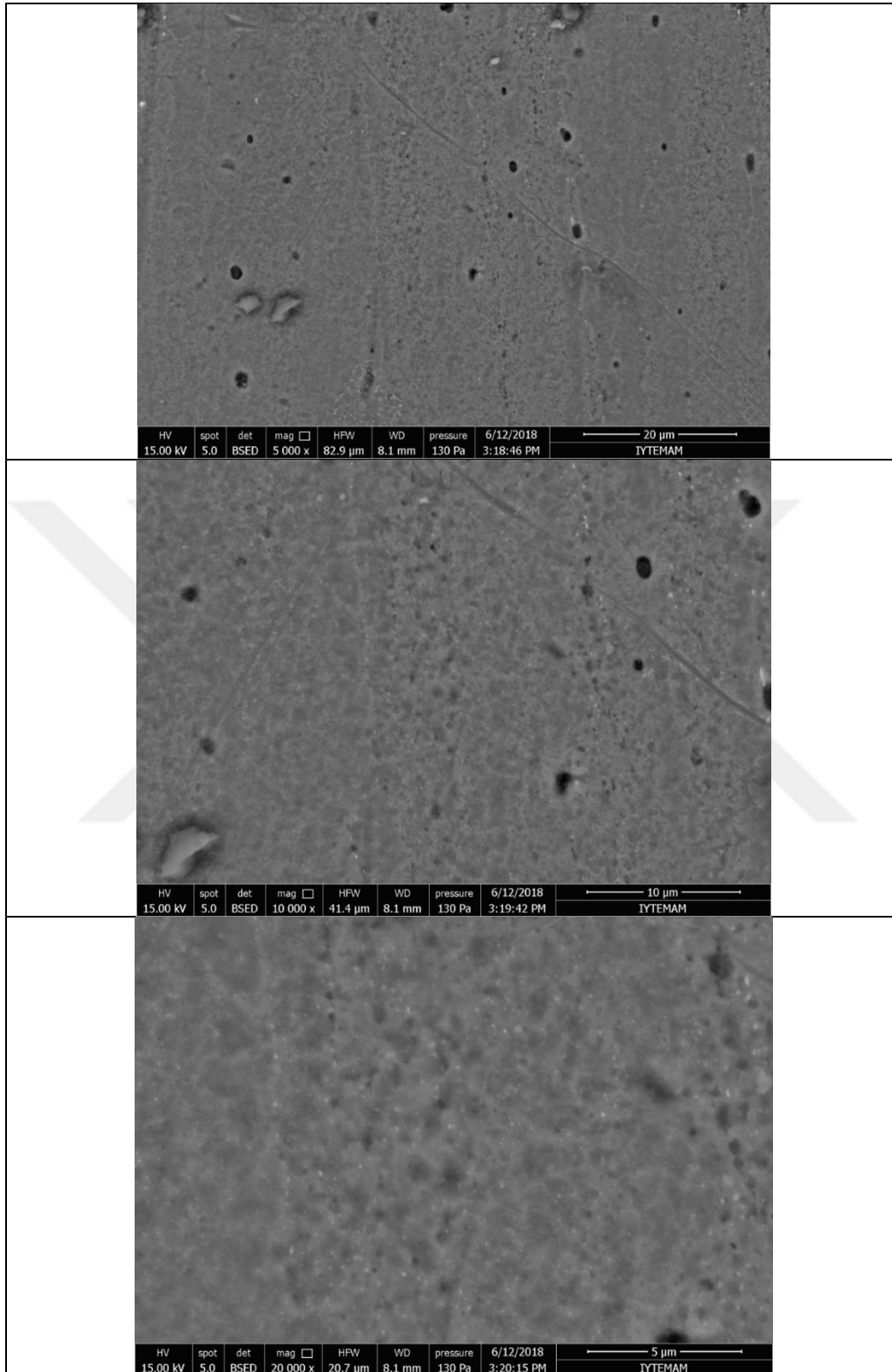
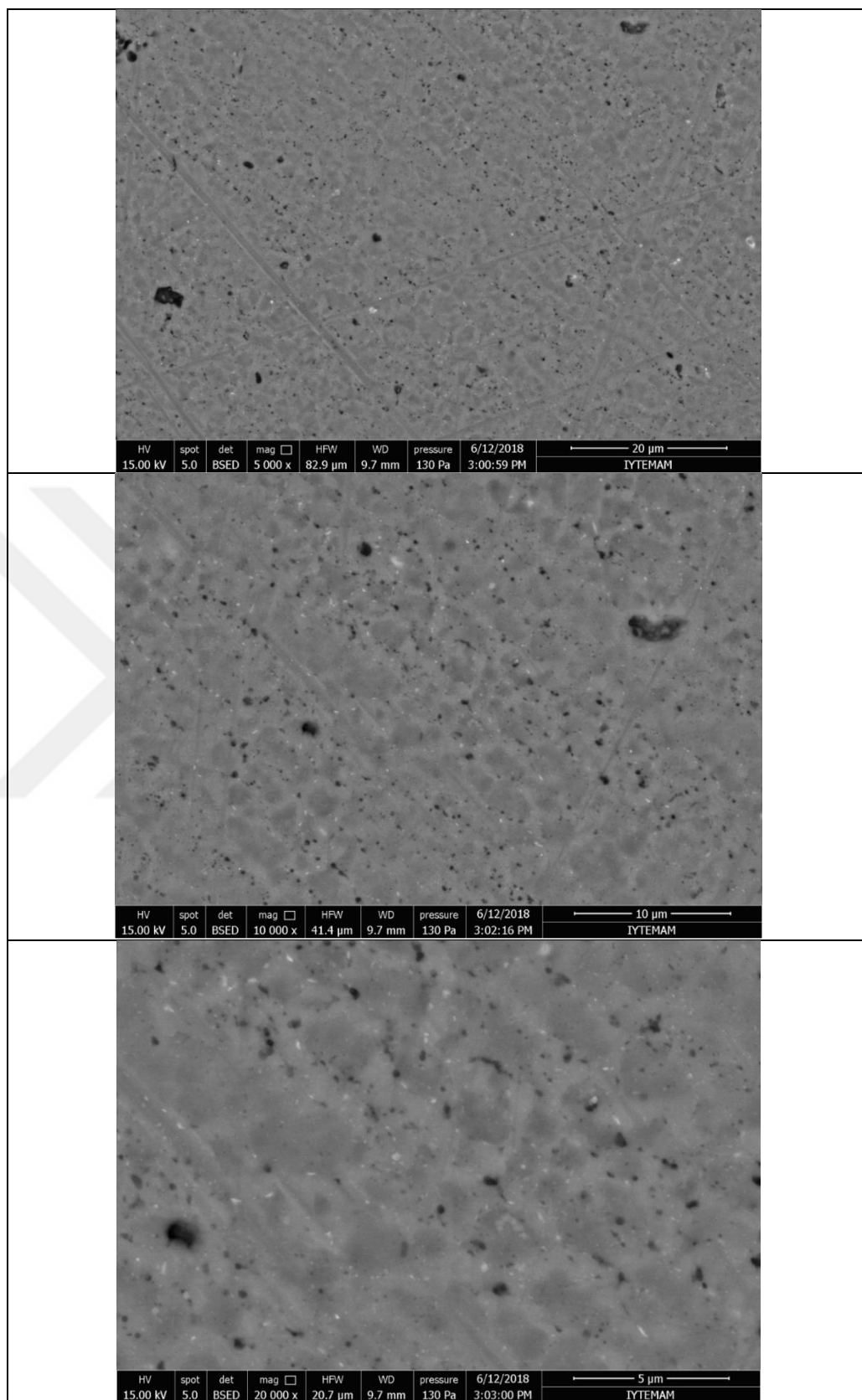**Figure A2.2 :** SEM images taken from C surface at different magnifications of no pass Al7075 samples.
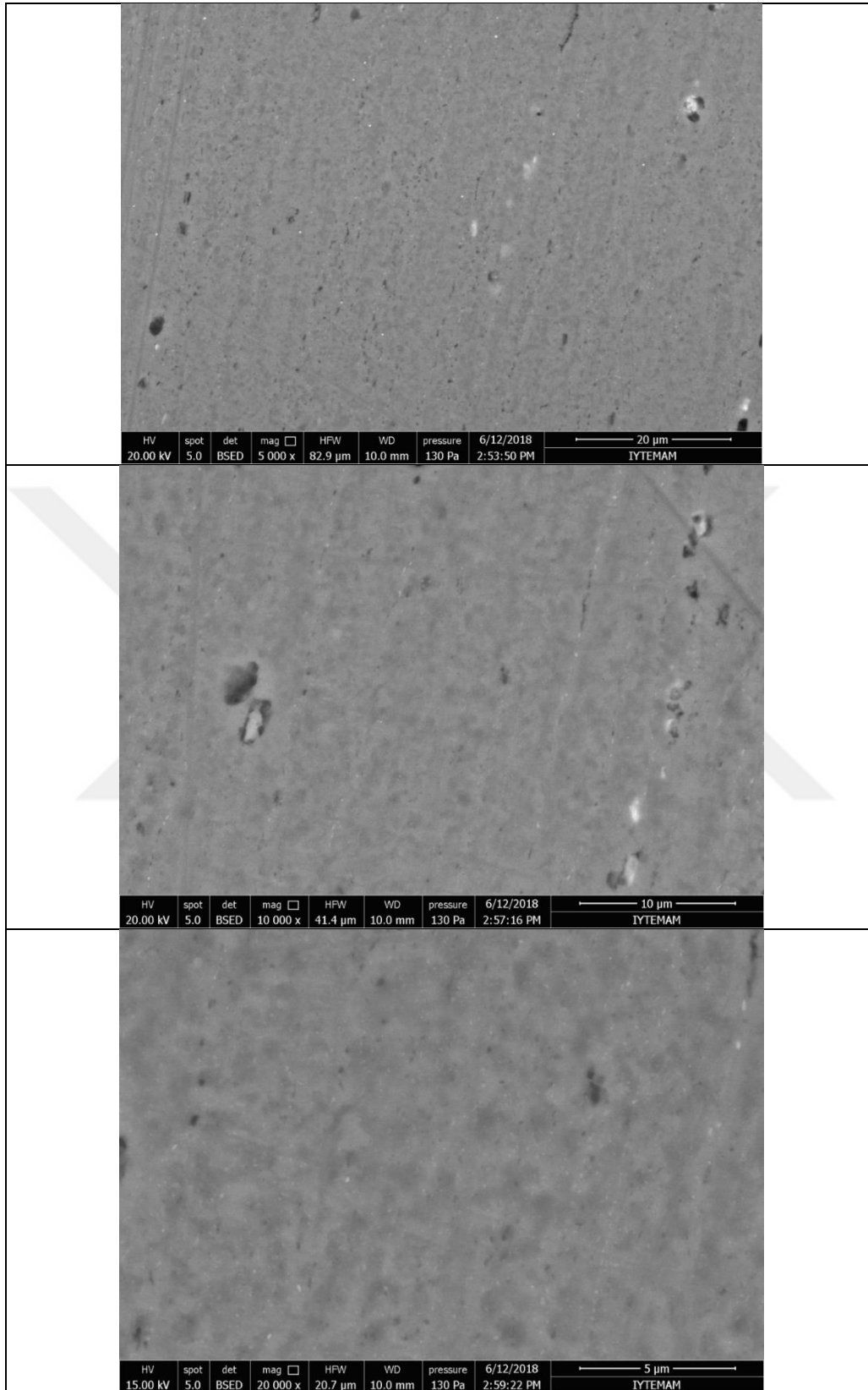
Figure A2.3 : SEM images taken from S surface at different magnifications of 2 passed Al7075 samples.

Figure A2.4 : SEM images taken from C surface at different magnifications of 2
passed Al7075 samples.

Figure A2.5 : SEM images taken from S surface at different magnifications of 4 passed Al7075 samples.
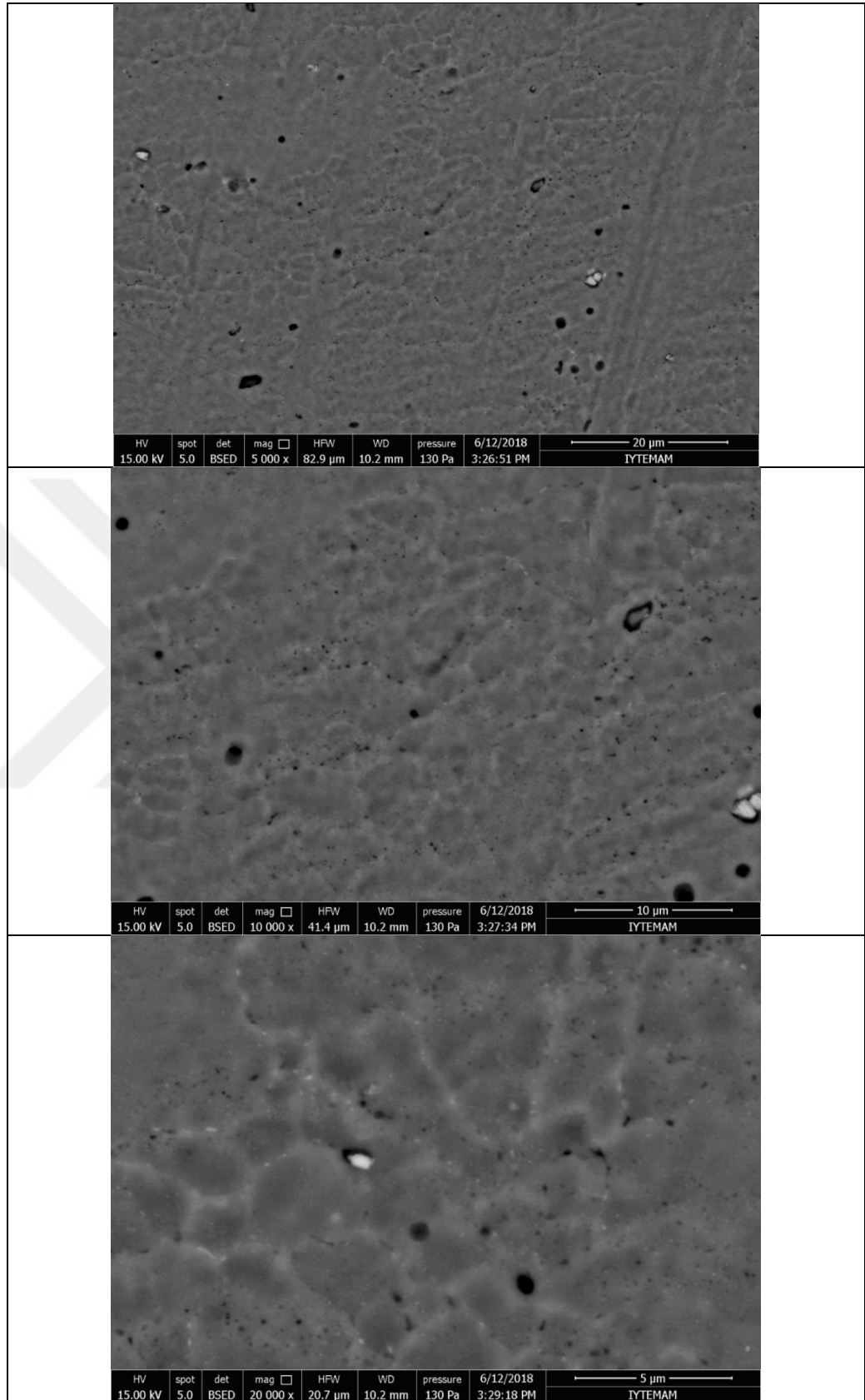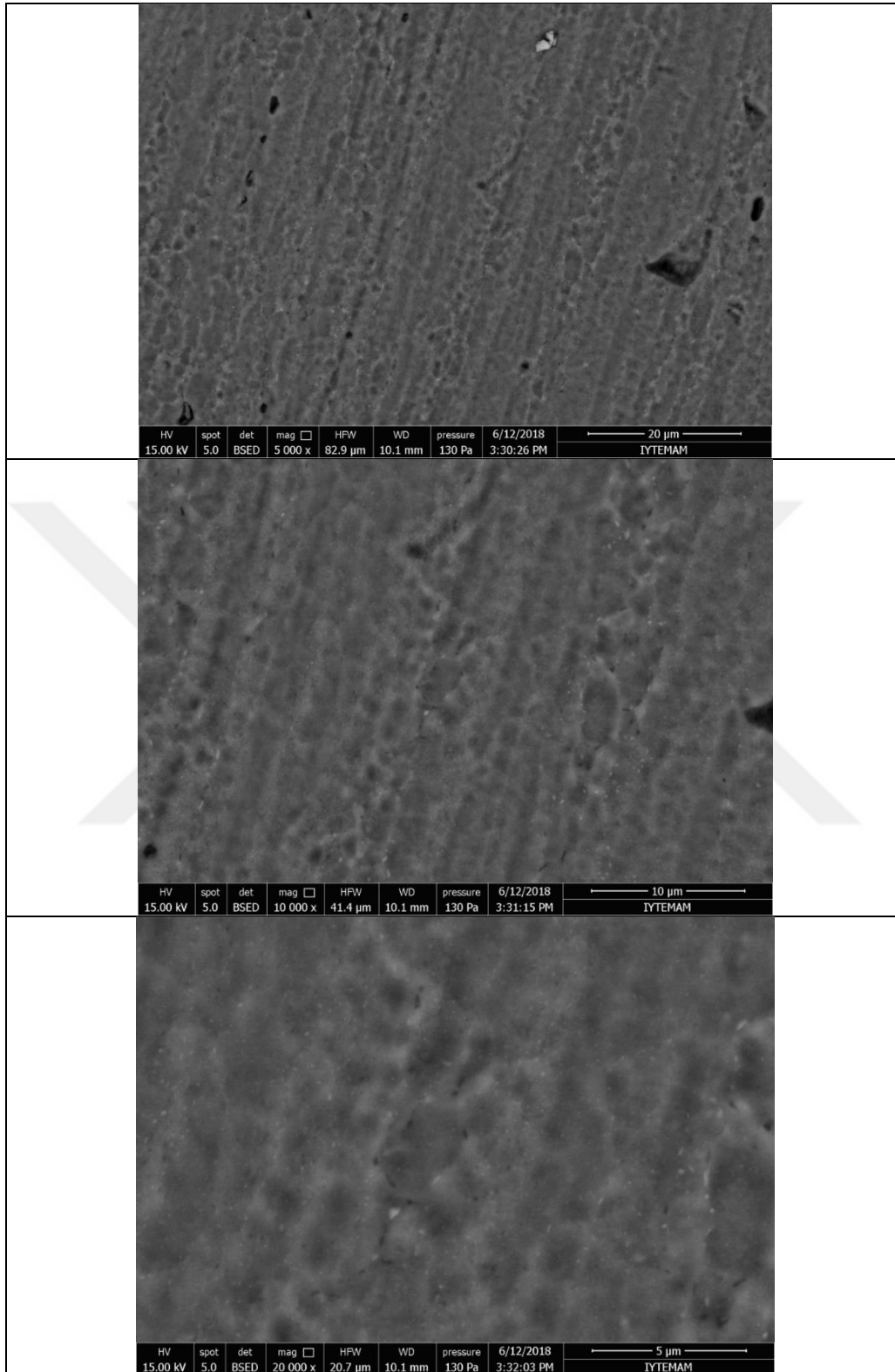
Figure A2.6 : SEM images taken from C surface at different magnifications of 4 passed Al 7075 samples.

Figure A2.7 : SEM images taken from S surface at different magnifications of 8 passed Al 7075 samples.

Figure A2.8 : SEM images taken from C surface at different magnifications of 8 passed Al 7075 samples.

CURRICULUM VITAE

Surname   :   Yeşil
First Name   :   Mehmet M.
Tel   :   +90 536 257 91 06
e-mail   :   mehmet.yesil@yahoo.com

Education and further studies :

- Middle East Technical University
   Mechanical Engineering Faculty
   Gaziantep campus
   Graduation date : 13 July 1992

- Autocad, Primavera Project Planner, MS Project Planner

- Pedagogical Formation __July-August 1993
   9 Eylül University / Izmir

- Basic Machine Training __5 April-28 May 1999
   General Directorate of Rural Services / Ankara

- Mercedes Truck Course__6-10 November 2000
   Rural Services Trainig Center / Mersin

- Cardio Pulmonary Respiration (CPR) & First Aid Training
   Bureau Veritas__26 June 2004
   GE Kemalpasa Site / Izmir

- General Electric (2004-2006)
Combined Cycle Power Plants
Izmir   :   Kemalpaşa Project
Mersin :   Camis Project
Rotterdam: Pergen Project
Engineered Equipment Package of the project consisting of :
GT Frame 9E and auxiliaries
GT Frame 6C and auxiliaries
270T652 ST,
GE Speedtronic Mark VI,
Generators including the requisite features and accessories,
HRSG made by NEM,
DCS by Yokogawa

Experiences :

Period	Employer	Activities-Responsibilities
July 1992-October 1993	ÖZTEKNİK Natural Gas Ankara	-Natural Gas and Central Heating, Cooling, Air Conditioning
October 1993-September 1997	Ministry of Education Uşak-Aksaray	-English&Computer Teacher -Central Heating Engineering
September 1997-October 2002	General Directorate of Rural Services Aksaray	-Hydraulic-Pneumatic Systems Design&Service -Quality Control Engineering
November 2002 – June 2011	University of EGE Izmir	-Heating, Cooling, Air Conditioning -Quality Control Engineering
June 2011–	İzmir Katip Çelebi University Izmir	-Heating, Cooling, Air Conditioning -Quality Control Engineering

List of Publications:

Conference Papers:

Characterization of Al7075 Alloy processed by Equal Channel Angular Pressing (ECAP), 2. International Students Science Congress (May 2018)